Current Pollution Reports (2022) 8:519–555
https://doi.org/10.1007/s40726-022-00238-3

WATER AND SEDIMENT POLLUTION (G TOOR, L NGHIEM AND W ZHANG, SECTION EDITORS)

Biochar Modification Methods for Augmenting Sorption of Contaminants

Abhishek Kumar[1] · Tanushree Bhattacharya[1] · Wasim Akram Shaikh[1,4] · Sukalyan Chakraborty[1] · Dibyendu Sarkar[2] · Jayanta Kumar Biswas[3]

Accepted: 24 September 2022 / Published online: 12 October 2022

Abstract

Biochar is a stable carbonaceous material obtained on pyrolysing biomass. Although it possesses crucial properties of high surface area, porosity, surface functionality, and sorption capacity, there is immense scope to augment these properties for effective contaminant sorption. Physical and chemical modifications enhance surface area, porosity, and contents of oxygen-containing functional groups. While acidic modifications augment surface functional groups and cation exchange capacity, alkaline modifications increase aromaticity, hydrophobicity, and π-π interactions. Impregnation with metals amplifies magnetic properties, availability of active sites, chemisorption, electrostatic attraction, and complexation. These modifications assist in sorption of cationic and anionic contaminants. Accordingly, the present study reviews modified biochars which promote eco-friendly contaminant removal. Moreover, various biomass and modification methods utilised for modified biochar production have been elaborated along with the changes in physico-chemical properties. Importantly, mechanistic insights into the functional role of modified biochars for removal of contaminants have been provided. Further, the impact of ageing on modified biochars and their contaminant adsorption performance have been discussed. Lastly, the feasibility and limitations of various biochar modification methods in addition to different research gaps have been presented to create a road map for future investigations. Waste management and contaminant remediation are the need of the hour for planet survivability, which could be achieved by precise biochar modification.

Keywords Biochar · Physical modification · Chemical modification · Metal impregnation · Removal mechanisms

Introduction

In the purview of increasing pollution levels, resulting from anthropogenic activities, and the consequent need to remove organic and inorganic contaminants, sorption has gained enormous attention primarily because of low operational costs, unsophisticated treatment, minimal chemical use, and safe handling of waste [1]. Previously, metal oxides, biomasses, and activated carbons have been used as sorbents with activated carbon being the most widely utilised sorbent in industries because of its high porosity, large surface area (SA), and abundant oxygen (O)-containing surface functional groups [2]. However, activated carbons are expensive while metal oxides could be toxic to the ecosystem which triggers the need for identifying potential alternatives. Lately, biochar has been reported to possess vital physicochemical properties such as high porosity, enhanced SA, alkaline pH, and O-containing functional groups, which

This article is part of the Topical Collection on *Water and Sediment Pollution*

✉ Tanushree Bhattacharya
tbhattacharya@bitmesra.ac.in

✉ Jayanta Kumar Biswas
jkbiswas@klyuniv.ac.in

[1] Department of Civil and Environmental Engineering, Birla Institute of Technology, Mesra, Ranchi, Jharkhand 835215, India

[2] Civil, Environmental, and Ocean Engineering Department, Stevens Institute of Technology, Hoboken, NJ, USA

[3] Department of Ecological Studies and International Centre for Ecological Engineering, University of Kalyani, Kalyani Nadia- 741235, West Bengal, India

[4] Department of Basic Sciences, School of Science and Technology, The Neotia University, Diamond Harbour Road, West Bengal 743368 Sarisha, India

enable sorption of contaminants [3–6]. Biochar is a stable carbon-rich material obtained on subjecting biomass to thermal energy in oxygen-deprived conditions [7–9]. It is used for applications ranging from agricultural amendment to industrial manufacturing and from energy production to waste management enabled by its vital properties such as alkaline pH, high SA, surplus porosity, enhanced water holding capacity, commendable sorption capacity (Qe), and abundant nutrients, which are dependent on biomass variation and preparatory conditions [7, 10–12].

Although biochar possesses crucial properties, there is huge scope to augment its properties for effective contaminant sorption to reduce pollution [2]. Biochar could be treated with steam for physical modification, while it could be treated with acid/alkali for chemical modification [13, 14]. Alternatively, biochar could be impinged with different materials such as metals, metal oxides, nanomaterials, or other waste materials to fabricate modified biochars [2, 10, 11, 15]. These modifications could be performed before or after thermal treatment of biomass to improve the surface morphology, physico-chemical property, and contaminant removal efficiency (RE) of modified biochar [2, 14]. Previously, reviews have been published for modified biochars mostly focussing on their removal efficiencies for anionic contaminants [2, 16–19], but holistic studies on contaminant removal potential are limited. Therefore, the present review focuses on (i) describing the various types of modification of biochars which remove organic and inorganic contaminants; (ii) elaborating different methods used for fabrication of modified biochars prepared using various biomass materials; (iii) providing a framework to understand the improvement in physico-chemical properties of modified biochars prepared via different modification techniques; (iv) facilitating insights into the mechanistic aspects of contaminant removal by modified biochars; and (v) presenting different limitations, challenges, and research gaps to provide a direction to future research investigations.

Physical Modification

Physical modifications are performed after biochar production by ball milling it or treating it with steam or heat or purged gas (Fig. 1; Table 1). Although physical modifications increase SA and porosity, they are not regarded to be highly effective in augmenting contaminant removal (especially anionic contaminants like As, F, nitrate, and phosphate), when compared to chemical modifications [20].

Steam-Modified Biochar

For steam treatment, superheated steam is passed (at 2.2–5 mL/min) through porous biochar at temperature range of 650–950 °C for 30–180 min [21, 22]. During the treatment, oxygen from steam is added to active sites on surface, while hydrogen forms complexes. Steam treatment initiates devolatilisation and removes particles trapped during incomplete combustion, which enhances its porosity and SA [19]. Steam reacts with biochar, thereby converting fixed carbon and volatile matter into CO and CO_2 resulting in pore formation [23]. Further, it oxidises the surface and increases O-containing functional groups (e.g. hydroxyl, carboxyl, carbonyl, phenol, and ether). Although steam is a weak oxidant, it increases hydrophilicity of biochar, which augments electrostatic repulsion with anionic contaminants and electrostatic attraction with cationic contaminants. Longer activation times enable larger contaminant removal. However, steam modification could be associated with limited increase in surface functional groups and repulsive forces between anions and surface, which could be disadvantageous [20, 24–26]. Further, steam modification decreases aromaticity, polarity, and H/C, N/C, and O/C ratio, which makes it less preferable to other treatments. Steam treatment augmented the SA of aegle shell (wood apple)-based biochar from 2.3 to 7.1 m^2/g, while the biochar removed ibuprofen with 95% efficiency [27]. Rajapaksha et al. [28] treated tea waste biochar with steam, which decreased its pH at 700 °C (from 11.05 to 10.48), eventually enabling a higher removal of sulfamethazine. In another study, Rajapaksha et al. [22] modified *Sicyos angulatus*-based biochar with steam, where pH at 700 °C decreased from 12.32 to 11.72, eventually facilitating higher sulfamethazine removal (increased from 20.56 to 37.73 mg/g after steam treatment) (Table 2). Lou et al. [25] modified pine sawdust with steam to remove phosphate from aqueous solutions, where steam treatment decreased pH from 4.92 to 4.82 at 300 °C and from 8.16 to 7.46 at 700 °C, which influences surface charge and Qe of biochar.

Purged Gas-Modified Biochar

Biochar is modified by purging CO_2/NH_3 gas, primarily to improve its SA and Qe. While CO_2 modification enhances SA and porosity (especially microporosity), NH_3 modification enriches surface with N-containing compounds. CO_2 purging also increases the activated sites on biochar surface. CO_2 modification increased the SA from 56.9 to 755.3 m^2/g in corncob-based biochar [29]. CO_2 reacts with C of biochar to form CO, resulting in formation of a microporous structure, which increases its sorption capacity [23]. The increase in SA, porosity, complexation (between graphitic-N and surface functional groups), and cation-π bonding enables contaminant sorption [30, 31]. Soybean straw–derived biochar was modified with both CO_2 and NH_3 to simultaneously improve the SA (up to 627.15 m^2/g) and nitrogen functional groups on surface, which eventually augments sorption capacity [32].

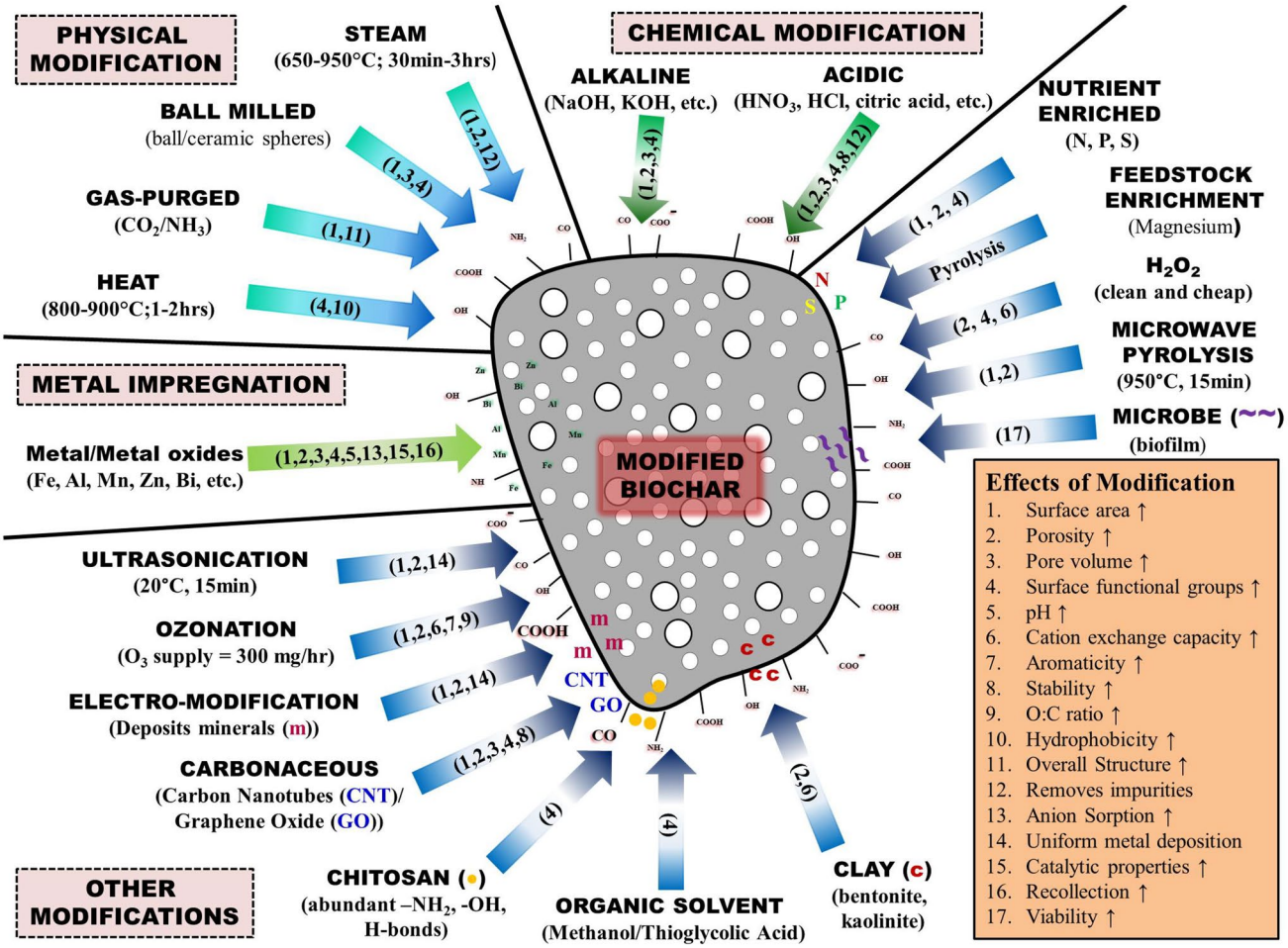

Fig. 1 Biochar modifications and their effects

Heat-Modified Biochar

During heat treatment, biochar is exposed to high temperatures (800–900 °C) for 1–2 h mainly to furnish basic surface functional groups to increase hydrocarbon sorption [33, 34]. Removal of hydrophilic groups (such as ether- or carbonyl groups) during heat treatment enhances surface hydrophobicity. Heat-treated biochars could be exposed to gases (such as hydrogen or argon) to form basic functional groups such as pyrone-type groups (arising from hydrophilic ether or carbonyl groups). Moreover, exposure to hydrogen deactivates active sites on surface by forming C–H bonds which stabilises and enhances basicity of biochar [33, 34].

Ball-Milled Biochar

Ball milling is a common technique to augment surface area of any substance by utilising the kinetic energy of moving balls of the instrument to break, grind, mix, and fabricate a material with physical and chemical modifications and an improved surface [35, 36]. It avoids the use of chemicals and is less energy intensive than conventional technologies such as microwave pyrolysis and laser ablation [37]. Ball milling reduces the particle size, increases the pore volume, increases the oxygen-containing surface functional groups, and modifies the surface chemical composition, which eventually augments the adsorption capacity of biochar [38]. The increase in pore volume exposes the graphitic structure of biochar, which enhances the cation-π action [35]. Spheres of dense ceramic materials such as yttria-stabilised zirconia could be utilised as grinding media, due to its chemical inertness, low wear and tear rate, and high reusability [39]. Salt-assisted milling is another ball milling method that utilises sodium chloride crystals along with yttria-stabilised zirconia, where salt crystals in conjunction with biochar is broken down into smaller pieces during milling; salt is later removed by dispersing the milled biochar in an aqueous media followed by centrifugation so that the salt remains in top layer [39]. Bamboo, bagasse, and hickory chip-based biochars were ball milled and high

Table 1 Physical modification of biochar

Feedstock; treatment	Target pollutant	Adsorption capacity or removal efficiency (RE)	Mechanism and other comments	Reference
Steam treated (activated)				
Mung bean husk; 550 °C pyrolysed; 650 °C steam activated	As	0.36 mg/g	Electrostatic attraction, chemisorption	[21]
Tea waste	Sulfamethazine	33.81 mg/g	High SA, CEC, π-π electron interactions, cation-π interactions	[28]
Sicyos angulatus (invasive plant)	Sulfamethazine	37.7 mg/g; 55%↑	Electrostatic interactions, chemisorption	[22]
Pecan shell	Cu	42.3 mg/g	Formation of Cu-humic acid-like organic-ligands, azurite-like carbonates, tenorite-like CuO	[41]
Pine sawdust; 300, 550 °C pyrolysed	Phosphate	<4%	Repulsion between phosphate and surface	[25]
Ascophyllum nodosum (seaweed)	Cu	223 mg/g	Cationic and anionic electrostatic attractions, surface precipitation, and pore depositions	[42]
Gas purged				
Cotton stalk; CO_2, NH_3	CO_2	99 mg/g (with CO_2)	CO_2-modification enhanced SA (~ 627.15 m^2/g rise), porosity; NH_3-modification enriched N-containing compounds (3.91%)	[30]
Corn straw; NH_3	Cd^{2+}	1.76 mmol/g	High graphitic-N content (46.4%), SA (418.7 m^2/g), complexation with graphitic-N, surface functional groups, cation-π bonding	[31]
	Cu^{2+}	1.63 mmol/g		
Heat treated				
Bamboo; heat, $KMnO_4$, HNO_3, NaOH	Furfural	100%	Increased hydrophobicity	[33]
Ball milled				
Coconut, pinenut and walnut shells; 500 °C pyrolysed; iron, iron oxide treated; ball milling (550 rpm for 6 h; quartz sand; rotation direction changed every 0.5 h)	Carbamazepine Tetracycline	62.7 mg/g 94.2 mg/g	Addition of quartz sand improved mechano-chemical degradation of pharmaceuticals	[43]
Sugarcane bagasse, bamboo, hickory wood chips; 300, 450, 600 °C pyrolysed; ball milling (300 rpm for 12 h; agate balls; rotation direction changed every 0.5 h)	Ni	26.7 to 396 mmol/kg	Strong cation-π interaction, electrostatic interaction, surface complexation	[35]
Hickory wood chips; 600 °C pyrolysed; CuO modified; ball milling (400 rpm for 9 h; agate balls; rotation direction changed every 1.5 h)	Reactive red 120	56.67 mg/g	Electrostatic interactions, chemisorption, intra-particle diffusion	[44]

**CEC* catio exchange, *SA* surface area

Table 2 Properties of modified biochars

Modification	Feedstock; pyrolysis (°C)	pH (unmodified biochar)	pH (modified biochar)	C (%)	Surface area (m^2/g)	Reference
Steam	Mung bean husk; 550 °C	NA	NA	NA	405	[21]
Steam	Tea waste; 300 °C	7.9	8.6	71.5	1.5	[28]
Steam	Tea waste; 700 °C	11.1	10.5	82.4	576.1	[28]
Steam	*Sicyos angulatus*; 300 °C	10.9	11.1	68.1	1.2	[22]
Steam	*Sicyos angulatus*; 700 °C	12.3	11.7	50.6	7.1	[22]
Steam	Pine sawdust; 300 °C	4.9	4.8	64.0	< 1	[25]
Steam	Pine sawdust; 550 °C	8.2	7.5	69.6	397.1	[25]
CO_2	Cotton stalk; 600 °C	NA	NA	NA	351.5	[30]
NH_3	Cotton stalk; 600 °C	NA	NA	NA	251.9	[30]
NH_3	Corn straw; 800 °C	NA	NA	77.6	418.7	[31]
Heat (800 °C)	Bamboo; 550 °C	NA	NA	70.7	494.2	[33]
KOH	Rice husk; NA	NA	NA	NA	1818.45	[62]
KOH	Cotton stalk; 400 °C	NA	NA	NA	60.3	[66]
NaOH	Rice straw; 400 °C	NA	NA	69.17	141.6	[68]
NaOH	Poplar wood; 400 °C	NA	NA	68.06	41.0	[68]
NaOH	Bamboo; 400 °C	NA	NA	80.32	8.3	[68]
H_3PO_4	Cotton stalk; 400 °C	NA	NA	NA	47.3	[66]
HNO_3	Cactus; 600 °C	NA	NA	NA	< 5	[83]
HCl	Reed; 300 °C	6.7	3.5	71.1	2.93	[84]
HCl	Reed; 400 °C	7.1	3.8	79.2	4.26	[84]
HCl	Reed; 500 °C	7.6	3.9	83.9	11.85	[84]
HCl	Reed; 600 °C	8.5	4.4	87.8	88.35	[84]
Acetic acid	Eucalyptus saw dust;120 °C	NA	NA	45.28	1.21	[59]
Tartaric acid	Eucalyptus saw dust; 120 °C	NA	NA	44.66	1.28	[59]
Citric acid	Eucalyptus saw dust; 120 °C	NA	NA	45.28	0.69	[59]
Fe	Wheat husk; 600 °C	8.3	7.0	36.84	339	[146]
Fe	Rice husk; 600 °C	6.8	5.5	38.39	300	[146]
Fe	Banana pith; 400 °C	NA	NA	49.40	31.59	[152]
Fe, KOH	*Guadua chacoensis*; 700 °C	4.0	10.9	10.62	482.4	[153]
Fe	Coconut, pinenut, walnut shells; 500 °C	NA	NA	NA	365	[43]
Al	Macro-algae; 450 °C	NA	NA	NA	45.46	[166]
Al	Rice straw; 600 °C	NA	NA	NA	186.95	[169]
Mn	Rice husk; 600 °C	10.89	6.72	40.8	42.9	[106]
Mn	Swine manure; 400 °C	NA	NA	NA	70.91	[170]
Mn	Corn straw; NA	10.0	11.0	73.4	80.3	[110]
Bi, HCl	Wheat straw; 400 °C	NA	NA	NA	87.42	[143]
Bi, HCl	Wheat straw; 500 °C	NA	NA	NA	190.40	[143]
Bi, HCl	Wheat straw; 600 °C	NA	NA	NA	106.70	[143]
Zn	Pig manure; 700 °C	NA	7.0	34.14	516.67	[113]
Zn	Sugarcane bagasse; 450 °C	NA	1.9	78.6	21.28	[117]
Zn	Crawfish shell; 450 °C	NA	NA	22.83	134.19	[174]
La	*Typha latifolia*; 500 °C	NA	5.6	42.31	8.11	[120]
La	Sodium alginate fibre; 900 °C	NA	NA	63.4	177.41	[179]
Mg, electro	Macroalgae; 600 °C	NA	NA	NA	56.42	[180]
Mg, electro	*Laminaria japonica*; 600 °C	NA	6.0	NA	386.5	[193]
Mg	*Cupressus sempervirens*; 600 °C	5.7	9.7	NA	35.0	[181]
Co	Bamboo; NA	5.8	3.1	NA	263	[126]

Table 2 (continued)

Modification	Feedstock; pyrolysis (°C)	pH (unmodified biochar)	pH (modified biochar)	C (%)	Surface area (m^2/g)	Reference
Ni	Bamboo; 500 °C	5.75	4.72	NA	263	[127]
Ca	*Laminaria japonica*; 200 °C	NA	8.31	40.81	2.39	[131]
Ca	*Laminaria japonica*; 400 °C	NA	11.40	46.50	17.72	[131]
Ca	*Laminaria japonica*; 600 °C	NA	11.62	53.25	79.95	[131]
Ca	*Laminaria japonica*; 800 °C	NA	12.59	60.51	45.46	[131]
Mg	Conocarpus green waste; 600 °C	NA	NA	NA	391.8	[137]
Fe	Conocarpus green waste; 600 °C	NA	NA	NA	260.5	[137]
Fe–Mn–La	Corn straw; 600 °C	8.93	6.83	54.8	12.2	[185]
Fe–Mn–Ce	Corn straw; 600 °C	8.93	9.64	28.8	46.6	[186]
Fe, microwave	Walnut shells; NA	NA	NA	NA	418	[241]
Microwave	Wheat straw; 950 °C	NA	NA	26.4	119.3	[191]
Ti, ultrasonic	Corncob; 550 °C	NA	NA	81.79	450.53	[195]
Ozone	Pine; 400 °C	7.30	5.28	71.31	NA	[199]
Graphene oxide	Water hyacinth; 300 °C	NA	NA	66.79	25.89	[242]
CNT, sodium dodecylbenzenesulfonate	Hickory; 600 °C	7.25	6.74	77.69	359	[203]
CNT, sodium dodecylbenzenesulfonate	Bagasse; 600 °C	6.94	6.72	84.3	336	[203]
Chitosan	*Eichhornia crassipes*; 600 °C	NA	NA	71.24	90.78	[204]
Clay	Bamboo; 300 °C	5.3	6.6	NA	9.84	[247]
Clay	Bamboo; 400 °C	5.3	7.1	76.05	19.93	[247]
Clay	Bamboo; 500 °C	5.3	7.6	NA	18.05	[247]
Clay	Cassava peel; 500 °C	NA	5.4	NA	402	[248]
H_2O_2	Pinewood; 400 °C	7.16	5.6	71.4	NA	[251]
Thioglycolic acid	Sugarcane bagasse; 600 °C	NA	4.7	NA	5.69×10^3	[220]

**CNT* carbon nanotubes

removal of sulfamethoxazole (100.3 mg/g) and sulfapyridine (57.9 mg/g) was observed [40].

Chemical Modification

During chemical treatment, alkali/acid is mixed with feedstock/biochar to enhance properties like porosity, SA, and surface functionality (Fig. 1; Table 3) [20, 45]. Exposure to acidic/alkaline solution oxidises the surface and influences ion exchange, Qe, and hydrophobic/hydrophilic properties [1].

Alkali-Modified Biochar

Typically, feedstock/biochar is soaked/suspended in different concentrations of alkaline reagents, such as sodium hydroxide (NaOH), potassium hydroxide (KOH), and calcium hydroxide ($Ca(OH)_2$), at 30–100 °C for 6–24 h (alkali strengths varying from 0.1 to 10 M), where base:biochar ratio is crucial in synthesising high-performance biochars [16, 46]. Alkaline treatments separate ashes and introduce O-containing groups, like –OH, on the surface and augment porosity and SA, which enhances RE [19]. Alkaline modifications facilitate higher H/C (stability) and N/C (basicity) and lower O/C (hydrophilicity), compared to acidic modifications. High N/C suggests greater N-containing surface groups, which increases basic properties of modified biochars [19]. NaOH modifications increase SA and porosity more than other alkaline modifications [16]. However, decrease in SA has also been reported in previous studies, where KOH modification decreased SA of hydrochar (0.4–1.8 m^2/g compared to 4.4–9.1 m^2/g of unmodified hydrochar), but significantly increased Cd Qe from 13.92–14.52 mg/g in unmodified to 30.40–40.78 mg/g in KOH modified [47]. KOH-modified bamboo/poplar-based biochar showed improved surface area (1555 m^2/g) and porosity (0.2950 cm^3/g), which facilitated sites for loading iron particles and removing Cr (Qe = 25.68 mg/g) [48]. Alkaline modification (NaOH) was more effective in adsorption of Ni (6.20 mg/g), Pb (44.64 mg/g), and Cd (0.65 mg/g) in comparison to acid modification (sulphuric and oxalic

Table 3 Chemical modification of biochar

Feedstock; treatment	Target pollutant	Adsorption capacity or removal efficiency (RE)	Mechanism and other comments	Reference
Alkaline treated				
Rice husk; KOH:biochar = 3:1	phenol	6.53 mg/g	High SA (1818 m^2/g), PV (0.90 cm^3/g), micro-porosity (93.3%)	[62]
	toluene	263.3 mg/g		
Grape pomace; KOH	Pb^{2+}	137 mg/g	Pb^{2+}-π interaction, chemisorption, ion-exchange	[63]
Sawdust, wheat straw, corn stalk; KOH	Cd	30.40–40.78 mg/g	O-containing aromatic functional groups (trend: corn stalk < wheat straw < sawdust)	[47]
Municipal solid waste; KOH	As(V)	30.9 mg/g	π-π electron interactions, proton exchange; increased SA (from 29.1 to 49.1 m^2/g) and PV (from 0.039 to 0.357 m^3/g); K_2O and K_2CO_3 formation separates carbon layers from surface consequently increasing SA, porosity	[64]
Mangosten fruit peel/exocarp; KOH, CO_2	Cu^{2+}	20 mg/g	High SA (367.10 m^2/g), porosity, chemisorption	[65]
Cotton stalk; KOH	As	90–99.5%	High porosity, SA; decreased particle size	[66]
Hickory wood; NaOH	Pb^{2+}	19.1 mg/g	High CEC, SA, surface functional groups	[67]
	Cd^{2+}	0.98 mg/g		
	Cu^{2+}	17.9 mg/g		
	Zn^{2+}	1.83 mg/g		
	Ni^{2+}	0.89 mg/g		
Bamboo, wood, rice straw; NaOH	Phenanthrene	42.9 mg/g	Removal of base-soluble carbon, high SA (4–38 times rise), hydrophobicity	[68]
Bamboo; NaOH	Methylene blue	606 mg/g	Surface functional groups (carboxyl, diethylenetriamine)	[69]
Cherry stones; NaOH	Iodine	343–996 mg/g	High PV (0.22–0.47 cm^3/g), SA (343–932 m^2/g), microporous structure (92–94% microporosity)	[70]
Bamboo; NaOH	Chloramphenicol	NA	Greater surface functional groups, π-π interactions	[71]
Pine chip; NaOH; N_2, O_2	Diclofenac, naproxen, ibuprofen	372, 290, 311 mg/g for N_2 modified; 214, 228, 286 mg/g for O_2 modified	Chemisorption	[72]
Pinus taeda; NaOH	Tannic acids	8.2–29.3%	Chemisorption, deficient hydrophobic interactions	[73]
	Humic acids	9.3–44.9%		
Pine chip; NaOH	Emerging contaminants- sunscreen compounds (benzotriazole, benzophene); endocrine-disrupting compounds (17 β-estradiol, bisphenol A)	> 50%	Trend: 17-β-estradiol > benzophene > bisphenol-A > benzotriazole	[74]

Table 3 (continued)

Feedstock; treatment	Target pollutant	Adsorption capacity or removal efficiency (RE)	Mechanism and other comments	Reference
Rice husk; KOH	Tetracycline	58.8 mg/g	Larger SA, O-containing functional groups, π-π interactions	[75]
Corn straw; KOH	Hg^{2+}	32.12%	O-containing functional groups	[76]
	Atrazine	46.39%		
Wood, chicken litter; KOH	Cu^{2+}	4.41 mg/g for wood; 13.4 mg/g for chicken litter	High SA (360 m^2/g for wood; 118 m^2/g for chicken litter), net positive charge	[20]
Coconut; NaOH	Methylene blue	916.26 mg/g	Larger SA (2885 m^2/g) compared to KOH treatment (1940 m^2/g) indicating lesser corrosivity	[77]
Alfalfa; NaOH	Tetracycline	302.37 mg/g	High SA (796.5 m^2/g), PV (0.09 cm^3/g); strong chemisorption	[78]
Potato stems, leaves; KOH	Ciprofloxacin	23.36 mg/g	More mesopores than raw biochar; hydrophobic interaction, hydrogen-bonding interaction, electrostatic interaction, and $\pi-\pi$ interaction	
Acid treated				
Cotton stalk; H_3PO_4	As	84–98%	High porosity, SA; decreased particle size	[66]
Rice straw; H_3PO_4	Pesticide	> 99.9%	Although PV (from 1.2 to 0.65 mL/g), SA (from 522.5 to 517.1 m^2/g) decreased, sorption increased	[79]
Jute (475 °C pyrolysed); H_3PO_4	As	55%	Increased micro-porosity, complexation	[24]
Prunus armeniaca; H_3PO_4	Pb^{2+}, Cd^{2+}, Ni^{2+}, naproxen, chlorophenols	> 95%; > 78 mg/g	Chemisorption; pore, film and particle diffusion; Phosphate/polyphosphate salt bridges increase C crosslinking thereby improving adsorption structure	[80]
Banana peel; H_3PO_4; hydrothermal carbonisation	Pb^{2+}	241 mg/g	Precipitation, cationic exchange, surface complexation; 30% treatment showed best results (lower pH, diminished acidic functional groups, enhanced carbonisation)	[58]
Pine tree sawdust (350, 500, 650 °C pyrolysed); H_3PO_4	Pb	69.27–74.61 mg/g	Surface sorption, phosphate precipitation; rise in SA (from 51 to 930 m^2/g), C-retention (from 50 to 70–80%), PV (from 0.046 to 0.558 cm^3/g), micropore (from 59 to 78.4–81.9%); insertion of P-O-P into carbon matrix assisted in micropore formation; decreased energy requirement for biomass decomposition	[81]

Table 3 (continued)

Feedstock; treatment	Target pollutant	Adsorption capacity or removal efficiency (RE)	Mechanism and other comments	Reference
Wood shavings, chicken litter; H_3PO_4	Cu^{2+}	68.6 mg/g for wood; 61.9 mg/g for chicken litter	High SA (851 m^2/g for wood; 538 m^2/g for chicken litter)	[20]
Cactus; HNO_3	Cu(II)	3.5 mol/kg	Inner-sphere, outer-sphere complexation	[82]
Cactus; HNO_3	U(VI)	210 mg/g	Inner-sphere complexation, surface carboxyl groups	[83]
Reed; HCl	Pentachlorophenol	100%	π-π interactions, reduced ash contents (from 29.5% to 11.8%) provided adsorption sites; increased SA (from 58.7 to 88.3 m^2/g)	[84]
Burcucumber (an invasive plant *Sicyos angulatus*); H_2SO_4	Sulfamethazine	182 mg/kg	Increased SA (from 2.31 to 571 m^2/g), chemisorption, diffusion	[57]
Eucalyptus saw dust; acetic, tartaric, citric acids	Methylene blue	29.94, 99.01, and 178.57 mg/g for acetic, tartaric, and citric acid treatment	Assisted by surface carboxyl groups; Citric and oxalic acids reduced SA from 1.57 to 1.21 m^2/g and 0.69 m^2/g, respectively	[59]
Spent coffee grains; citric acid	Pb^{2+}, Cu^{2+}	0.77 mmol/g for Pb^{2+}, 1.53 mmol/g for Cu^{2+}	Enhanced carboxylic groups (from 0.47 to 2.2 mmol/g)	[51]
Corn straw; H_3PO_4	Cr Bisphenol A	116.28 mg/g 476.19 mg/g	Cr mainly adsorbed via chemical complexation, while organic pollutants through π-π interaction	[85]

**CEC* cation exchange capacity, *PV* pore volume, *SA* surface area

acid) [49]. Similarly, alkali modification in corn stalk-based biochar improved enrofloxacin removal more (54.08%; 58.29 mg/g) than acid modification (27.80%; 41.91 mg/g), primarily assisted by 14 times increase in SA in alkali modification (10 times rise in acid modification) [50].

Acid-Modified Biochar

Generally, feedstock/biochar is soaked/suspended in acidic reagents (with ratios up to 1:10 *w*:*v* ratio), like hydrochloric acid (HCl), sulphuric acid (H_2SO_4), and weak acids (e.g., citric acid) at 30–120 °C for several hours/days (acid strengths varying from 0.1 to 2.5 M) [16, 51–53]. Acid treatments remove residues of metals and impurities, and increase stability, regeneration, and RE by augmenting SA, microporosity, electrostatic interactions, and surface functionality (hydroxylic, carboxylic, carbonylic, phenolic, lactonic, and ketonic). H_2SO_4 and H_3PO_4 activation increased SA by 80% and microporosity by 263% in pork bone–derived biochar [54]. Acid-modification augments SA less than other modifications due to the breakdown of porous structures and expansion of micro-pores into meso-/macropores. Sahin et al. [55] compared the effect of acid treatments on poultry manure–derived biochar before and after pyrolysis conditions. While in pre-treatment, biochar pH decreased from 9.38 to 8.57 and 9.14 for H_3PO_4 and HNO_3 treatments, respectively, in post-treatment biochar pH decreased to 5.39 and 4.46 for H_3PO_4 and HNO_3 treatments, respectively, suggesting that acid treatment after pyrolysis significantly decreased the pH which could be beneficial for alkaline calcareous soils (Table 2). Yakout et al. [56] observed decrease in SA from 71.4 to 56.9 m^2/g in rice straw–based biochar after H_2SO_4 modification. Acid treatment could enhance density of bio-sorbents, which could diminish its Qe [1]. The diminished C content and enhanced O content and acidic surface functional groups increase H/C and O/C of acid-modified biochars [33, 57]. Biochars treated with 30% H_3PO_4 (among 0–50%) showed best sorption results, suggesting importance of its optimisation [58]. Spent sorbents could be reused by using 0.1 N HCl for removing contaminants [59]. Rice husk–derived biochar-supported sulphidated nano-zerovalent iron was pre-treated with HCl, NaOH, and H_2O_2 to improve nitrobenzene reduction performance and observed HCl-modified composite to be the most effective sorbent (100% removal at 200 mg/L in 60 min), probably assisted by negative surface charge, increased acidic functional groups, high surface area, and enhanced electron transfer rate [60]. Acid and alkaline treatments were compared by Mahdi et al. [61] using date seed–based biochar (550 °C pyrolysed), who reported acid pre-treatment to be most effective in greater removal of contaminants (Qe of 0.91 mmol/g, 0.71 mmol/g, and 0.69 mmol/g for Pb, Cu, and Ni, respectively).

Impregnated Biochars

Generally, chemical and physical treatments facilitate biochar with low sorption capacities. Correspondingly, biochar composites have been prepared with enhanced properties including new functional groups and high SA [17]. Typically, their preparation involves pre-/post-processing stages including immersion of feedstock/biochar into solutions of metal oxides or metals (e.g., Fe, Al, Mn, Bi, Zn, and others) (Fig. 1; Table 4), which deposits metals in pores and on surface of biochar, provides positive charge, and enhances RE [2]. Generally, these impregnations improve porosity, SA, surface functionality, and H/C, O/C, and N/C ratios [86]. The increase in surface area result from the accumulation of minerals on surface [87]. Metal impregnation could be combined with physical/chemical modifications to harness additional benefits of multiple treatments for improving the contaminant removal efficiency, as demonstrated in several previous studies (Table 4).

Fe-Modified Biochar

Iron modified biochars are the most studied biochars, primarily due to their magnetic properties (easy recollection) and the strong interaction between Fe and surface functional groups. Fe modification is achieved by soaking biomass/biochar in $FeCl_3$, $Fe(NO_3)_3$, $FeSO_4$, or Fe_3O_4. Pre-treatment is more effective in removing contaminants than post-treatment (due to Fe transformation into more complex crystalline phases) [88]. Pre-treatment with HNO_3 helps increase hydrophilicity, aiding in vertical growth of iron oxide on the surface and shortening the distance needed for contaminant diffusion in biochar, thereby improving its Qe [89]. Qe also depends on the type and/or structure of iron oxide (Qe-amorphous > crystalline) [90]. Fe modification at high pH and high pyrolysis temperature favours higher Qe [91]. Iron oxide is converted to zero-valent iron (ZVI) during pyrolysis/modification ($Fe_2O_3 \rightarrow Fe_3O_4 \rightarrow FeO \rightarrow Fe^\circ$), affecting biochar's properties and Qe [92]. Fe-modified biochar oxidises As(III) to As(V), and the removal is assisted by precipitation, surface sorption, electrostatic interaction, and inner-sphere complexation [93]. A rise in magnetic property of biochar could decrease its Qe. Anyika et al. [94] reported $FeCl_3$-modified palm kernel shell-derived biochar with significant magnetic property (saturation magnetisation—49.5 emu/g) but low contaminant sorption (Qe = 0.054 mg/g), while Lunge et al. [95] suggested $FeCl_3$-modified tea waste–derived biochar, with low saturation magnetisation (6.9 emu/g) and high Qe. Nevertheless, Dhoble et al. [96] fabricated $Fe(NO_3)_3$-modified

Table 4 Metal impregnation

Feedstock; treatment	Target pollutant	Adsorption capacity or removal efficiency (RE)	Mechanism and other comments	Reference
Wheat, rice husk; co-pyrolysis with $FeCl_3$ (600 °C)	As	100%	Fe_3O_4 enabled As removal; mono-dentate, bi-dentate surface complexes	[146]
Rice straw; $FeCl_3$	As(V)	> 46%	Fe transformation into complex crystalline phases	[88]
	Cd(II)	> 50%		
Rice husk, municipal solid waste; $FeCl_3$	As	58–95%	Electrostatic interactions, co-precipitation (between As and $Fe(OH)_3$)	[147]
	Cr	14–89%		
Bamboo; chitosan, ZVI	Pb	93%	Chitosan (without ZVI) enhanced amine groups which escalated Pb^{2+}, Cr^{6+}, methylene blue removal (assisted by complexation, reduction, surface adsorption) but inhibited anion removal; ZVI increased electrostatic attraction, anionic sorption	[148]
	Cr	40%		
	As	95%		
	P	96%		
	Methylene blue	68%		
Water hyacinth; $FeCl_2$, $FeCl_3$ (250, 400 °C pyrolysed)	As(V)	> 90%; 7.41 mg/g	Enhanced interaction between OH^- and As	[91]
Oak wood, bark (fast pyrolysis 400–450 °C); Fe^{3+}/Fe^{2+}, NaOH	Cd, Pb	Oak bark (Pb—30.2 mg/g; Cd—7.4 mg/g); oak wood (Pb—10.13 mg/g; Cd—2.87 mg/g)	Electrostatic attraction; abundant functional groups; high SA	[145]
Bagasse, bamboo, tyre; $Fe(OH)_3$	Pb	86.6%, 93.8%, 94.9% for bamboo, bagasse, tyre	Enriched functional groups; metal precipitation with carbonates, phosphates; positively charged particles (silvite, periclase, dolomite, calcite) in mineral enhance phosphate removal	[149]
	PO_4^{3-}	71.7% for bagasse, 61.5% for bamboo		
	Cu	70.4%, 70.1%, 70.3% for bagasse, bamboo, tyre		
	Hg	77%, 66%, 83.4% for bagasse, bamboo, tyre		
Hickory chips (600 °C pyrolysed); $Fe(NO_3)_3$	As	2.16 mg/g	Chemisorption, O-containing groups	[150]
Corn cob; $Fe(NO_3)_3$	As	2.26 mg/g	Enhanced SA, PV	[151]
	Eu	0.98 mg/g		
Grape seed; pre-treated (HNO_3), post-treated ($Fe(NO_3)_3$)	As	34.9 mg/g	Enhanced SA, PV, Qe (~7 times)	[13]
Banana pith; $Fe(NO_3)_3$	As(V)	100%	Fe modification, eight times larger SA (31.59 m^2/g)	[152]
Guadua chacoensis (bamboo); KOH, $FeCl_3$, $FeSO_4$	As(V)	100% (868 mg/g)	Strong affinity with Fe	[153]
Coconut, pinenut, walnut shells; Fe_3O_4 ball milling	Carbamazepine	62.7 mg/g	Affinity between Fe_3O_4 and $–CONH_2$, –OH, $–N(CH_3)_2$; hydrophobic interaction, π-π interaction	[43]
	Tetracycline	94.2 mg/g		
Bamboo; Fe_3O_4	Polycyclic aromatic hydrocarbons	86%	Increased degradation efficiency due to redox coupling (Fe^{2+}–Fe^{3+}), electron transfer of functional groups (promotes sulphate generation)	[154]
Corn straw; Fe treated	P	> 99%	Enabled by Fe_3O_4	[155]

Table 4 (continued)

Feedstock; treatment	Target pollutant	Adsorption capacity or removal efficiency (RE)	Mechanism and other comments	Reference
Pine bark; $CoFe_2O_4$	Pb^{2+}	3.3 mg/g	Chemisorption	[156]
	Cd^{2+}	2.9 mg/g		
Pinewood; hematite	As	429 mg/kg	Electrostatic interactions with surface γ-Fe_2O_3	[157]
Wood chips, coconut shells; $FeSO_4.7H_2O$, $FeCl_3.6H_2O$ (Fe_2O_3 impregnated)	Pb	17,698 mg/kg	High SA	[158]
	Cu	2206 mg/kg		
	Phenol	20,695 mg/kg		
Empty fruit bunch, rice husk; Fe(III)	As(III), As(V)	empty fruit bunch (31.4 mg/g for As(III), 15.2 mg/g for As(V)); rice husk (30.7 mg/g for As(III), 16.0 mg/g for As(V))	O-containing groups, zeta potential, O/C ratio, polarity index [(O + N)/C]	[159]
Empty fruit bunch; $FeCl_3$:biomass = 1:2; microwave heating (20 min radiation time, 900 W microwave power)	Methylene blue	99.9% (265 mg/g)	High SA (890 m^2/g)	[160]
Cotton stalk; ferric oxides	Phosphate	0.963 mg/g	Increased SA, PV	[102]
Cottonwood (600 °C pyrolysed); $FeCl_3$/or hematite	As	3525 mg/kg	Electrostatic interactions	[161]
Paper mill sludge; magnetite rich; pyrolysed with CO_2	As	23.1 mg/g	High FeO, Fe_3O_4, $CaCO_3$ concentrations	[162]
	Cd	41.6 mg/g		
Paper mill sludge; Ni-ZVI	Pentachlorophenol	97.5%	Dechlorination, adsorption; bio-sorbents used for brick preparation (high compressive strength, minimal leaching of sorbed contaminants)	[163]
Rice hull; nano-ZVI	Trichloroethylene	99.4%	O-containing groups, large SA	[164]
Macro-algae; Fe_3O_4 (electro-magnetisation)	Acid orange	382.01 mg/g	Improved porosity, SA (337 m^2/g), magnetic properties	[165]
Macro-algae; stirred in Al electrode-based electrochemical treatment (450 °C pyrolysed)	Phosphate	31.28 mg/g	Nano-Al crystals (beohemite, AlOOH) assists removal	[166]
Cottonwood; $AlCl_3$ (600 °C pyrolysed)	As	17.4 mg/g	AlOOH nanocomposite has larger SA	[167]
Cottonwood; $AlCl_3$ (600 °C pyrolysed)	Methylene blue	85.0 mg/g	AlOOH nanocomposite has larger SA	[167]
Rice, peanut, soybean; $AlCl_3$	Phosphate	135.0 mg/g	Positively charged surface, increased SA	[168]
	As(V)	445–667 mmol/kg		
Rice straws; Al-rich red-mud mixed (600 °C pyrolysed)	As(V)	5.92 mg/g	Surface complexation, electrostatic interaction between As and iron oxides (hematite, magnetite), aluminium oxides (gibbsite)	[169]
Rice husk; birnessite-loaded ($KMnO_4$ precipitation)	As(III)	3.54 mg/g	Greater vacant sites; synergistic reactions between cations and anions; high co-adsorption ability; $Cd_3(AsO_4)_2$ precipitate formation; complexation with functional groups	[106]

Table 4 (continued)

Feedstock; treatment	Target pollutant	Adsorption capacity or removal efficiency (RE)	Mechanism and other comments	Reference
Rice husk; birnessite-loaded ($KMnO_4$ precipitation)	As(V)	2.41 mg/g	Greater vacant sites; synergistic reactions between cations and anions; high co-adsorption ability; $Cd_3(AsO_4)_2$ precipitate formation; complexation with functional groups	[106]
Swine manure; MnO_2	Cd	9.07 mg/g		[170]
	Pb	268.0 mg/g		
Swine manure; MnO_2	Cd	45.8 mg/g	Electrostatic interaction, ion exchange; high functional groups, PV, SA	[170]
Corn straw; nano-MnO_2 (via $KMnO_4$ reduction by ethanol)	Cu^{2+}	142.02 mg/g	Complexation (such as COO–Cu, Mn–O–Cu)	[110]
Pine wood; $MnCl_2.4H_2O$, birnessite	As	0.59 mg/g for $MnCl_2$; 0.91 mg/g for birnessite	Strong affinity with crystals	[105]
Pine wood; $MnCl_2.4H_2O$, birnessite	Pb	4.91 mg/g for $MnCl_2$; 47.05 mg/g for birnessite	Strong affinity with crystals	[105]
Hickory wood; $KMnO_4$ (600 °C pyrolysed)	Pb^{2+}	153.1 mg/g	MnO_x ultrafine particles assists removal; Augmented SA (from 101 to 205 m^2/g), surface O-containing groups	[87]
Hickory wood; $KMnO_4$ (600 °C pyrolysed)	Cu^{2+}	34.2 mg/g	MnO_x ultrafine particles assists removal; Augmented SA (from 101 to 205 m^2/g), surface O-containing groups	[87]
Pine wood; MnO_2	Cd^{2+}	28.1 mg/g		[171]
	Pb^{2+}	98.9%	Surface hydroxyl groups	
Corn straw; $KMnO_4$	Cu^{2+}	160 mg/g	Inner-sphere complexation of MnO_x, MnOH with O-containing groups	[86]
Grape stalk; MnO_2	Pb	99%	Precipitate formation	[172]
Grape stalk; MnO_2	As	91%	Precipitate formation	[172]
Wheat straw; Bi_2O_3, HCl; sonication; 400, 500, 600 °C pyrolysed	Cd	51%	High SA, porosity; ligand exchange (Lewis acid–base reaction) between Bi and contaminants	[143]
	Cr	12.2 mg/g		
Wheat straw; Bi_2O_3, HCl; sonication; 400, 500, 600 °C pyrolysed	P	16.2 mg/g	High SA, porosity; ligand exchange (Lewis acid–base reaction) between Bi and contaminants	[143]
	As	125 mg/g		[173]
Wheat straw; $Bi(NO_3)_3.5H_2O$, HCl (stirred—3 h, 80 °C), dried (200 °C), pyrolysed (400, 500, 600 °C); $NaHCO_3$ washed	As	22.4 mg/g	Reduction of iron oxides and enhanced Fe(II) concentration; rise in Fe(II) transports As from surface into pores	
Pig manure; KOH, NaOH, $AlCl_3$, $FeCl_3$, $ZnCl_2$	As	26.6 mg/g	Maximum Qe for $ZnCl_2$-modified biochar (SA = 516.7 m^2/g; porosity = 0.24 cm^3/g); Zn–OH forms Zn–O–As(III) by ligand exchange	[113]
Sugarcane bagasse; Zn	Cr(VI)	102.66 mg/g	functionalised with COO– groups; high porosity	[117]
Crawfish shell; $ZnCl_2$; 450 °C pyrolysed	As	17.2 mg/g	High SA, porosity due to fabrication of ZnO nanoparticles; enhanced surface positive charge	[174]
Pine cone; Zn	As	10.4 µg/g	Metal–ligand complexation	[175]

Table 4 (continued)

Feedstock; treatment	Target pollutant	Adsorption capacity or removal efficiency (RE)	Mechanism and other comments	Reference
Rice hull; ZnS nanocrystal; ferric acetylacetonate	Pb^{2+}	367.65 mg/g	Chemisorption	[176]
Pine cone; $Zn(NO_3)_2$	As	7 μg/g	Boundary layer diffusion, intra-particle diffusion	[177]
Opuntia ficus indica; $ZnCl_2$	As	8 mg/g	Presence of zinc; surface assistance	[178]
Typha latifolia (cattail plant); La	Phosphate	36.06 mg/g	Electrostatic attraction, ligand exchange, complexation	[120]
Sodium alginate fibre (wet spinning technology); La	Cr	104.9 mg/g	Electrostatic interaction, complexation, ligand exchange	[179]
Macroalgae; $MgCl_2$ dipped; electrochemically modified (20 V; 10 min)	Phosphate	620 mg/g	Periclase (MgO) nanocomposite	[180]
Cupressus sempervirens (cypress); $MgCl_2$	Pb	202.2 mg/g	High porosity, SA, high pH_{ZPC}, appreciable surface O-containing functional groups, lead precipitate formation (with inorganics)	[181]
Peanut shells, pine woods, cottonwoods, sugarcane bagasse, sugar beet tailings (600 °C pyrolysed); $MgCl_2.H_2O$	Phosphate	835 mg/g	Greater MgO content (8.3–26.1%)	[182]
Peanut shells, pine woods, cottonwoods, sugarcane bagasse, sugar beet tailings (600 °C pyrolysed); $MgCl_2.H_2O$	Nitrate	95 mg/g	Greater MgO content (8.3–26.1%)	[182]
	Fe^{2+}	84.6–99.8%	More than unmodified biochar (38.3–97.6%), zeolite/clinoptilolite (12.3–95.5%)	[183]
Conocarpus; $Mg(OH)_2$				
Wheat straw; NaOH, $MgCl_2$ ($Mg(OH)_2$ coated)	Anionic frozen yellow dye	167.5 mg/g	Electrostatic interaction; 98% regeneration	[184]
Bamboo; HNO_3, $Co(NO_3)_2$; microwave irradiation (Co coated)	Cr^{6+}	45.45 mg/g	Chemisorption; high PV (0.27 cm^3/g), SA (263 m^2/g)	[126]
Camellia oleifera shells; $Co(NO_3)_2{\cdot}6H_2O$, $Gd(NO_3)_3{\cdot}6H_2O$; HCl, ethanol	Ciprofloxacin	44.44 mg/g	Chemisorption; high SA (370.3737 m^2/g), PV (0.1991 cm^3/g)	[144]
Camellia oleifera shells; $Co(NO_3)_2{\cdot}6H_2O$, $Gd(NO_3)_3{\cdot}6H_2O$; HCl, ethanol	Tetracycline	119.05 mg/g	Chemisorption; high SA (370.3737 m^2/g), PV (0.1991 cm^3/g)	[144]
Bamboo; Ni	Pb^{2+}	142.7 mg/g	Increased SA (from 15.5 to 263 m^2/g), PV (from 0.105 to 0.270 cm^3/g); decreased pore size (from 15.2 to 4.11 nm)	[127]
Sugarcane bagasse; $NiCl_2$, N-doped CNTs; KOH	Cr	824.4 mg/g	High porosity (micropores, mesopores), surface precipitation	[128]
Rice straw; Ca-modified (Fe_3O_4, $CaCO_3$)	As, Cd	6.34 mg/g for As, 10.07 mg/g for Cd	Electrostatic interaction, surface complexation	[130]
Laminaria japonica; alginate, $CaCl_2$	Phosphate	97.02%	Intra-particle diffusion, external mass transfer mechanisms, high Mg/P, Ca/P ratios	[131]
Rice husk; CaO	As	> 95%	Chemisorption, metal precipitation, electrostatic interaction	[147]

Table 4 (continued)

Feedstock; treatment	Target pollutant	Adsorption capacity or removal efficiency (RE)	Mechanism and other comments	Reference
Rice husk; CaO	Cr	20%	Chemisorption, metal precipitation, electrostatic interaction	[147]
Conocarpus green waste; MgO, iron oxide	Nitrate	89% (45.36 mmol/ kg)	Chemisorption, complexation, high SA	[137]
Rice husk; polydopamine (hydrophilic polymer), nano-ZVI	Tetracycline	99.16%	Improved hydrophilicity; large SA	[139]
Corn straw; $Fe(NO_3)_3$, $KMnO_4$, $LaCl_3$	As	28.4 mg/g	Fe–O–As complex formation (aided by FeO, Fe_2O_3, FeOOH), electrostatic attraction, inner-sphere La–O–As complex formation (enabled by La–O), MnO_2-assisted As oxidation	[185]
Corn straw; $Fe(NO_3)_3$, $KMnO_4$, $Ce_2(CO_3)_3$	As	8.74 mg/L	Surface sorption, As oxidation; mono-dentate and bi-dentate complexation with –OH	[186]
Corn stem; Fe and Mn oxides	As	8.25 mg/g	Assisted by Fe–Mn oxides, chemisorption, As interaction with O-rich functional groups	[187]
Rice husk; $KMnO_4$, $Fe(SO_4)_2$, humic acid	As	35.5 mg/g	Covalent bonds involved in As sorption; chelation, deposition involved in Cd removal	[188]
Rice husk; $KMnO_4$, $Fe(SO_4)_2$, humic acid	Cd	67.11 mg/g	Covalent bonds involved in As sorption; chelation, deposition involved in Cd removal	[188]
Pine (*Pinus taeda*); Ni/Mn oxide (pre-pyrolysis); Ni/Mn-layered double hydroxides (post-pyrolysis)	As	0.549 and 6.52 mg/g for Ni/Mn oxide and Ni/Mn-layered double hydroxides	Anion exchange, surface complexation; post-treatment 12 times more effective in removal; efficient removal even after 3 desorption cycles	[189]

**CEC* cation exchange capacity, pH_{zpc} pH at point of zero charge, *PV* pore volume, *SA* surface area, *ZVI* zero-valent iron

bark-based biochar with high saturation magnetisation (38.6 emu/g) and superior As(III) affinity (enabled by inner- and outer-sphere complexation), compared to As(V) (only inner-sphere complexation). Corn straw–derived biochars were modified with Fe to compare pre-treatment ($FeCl_3.6H_2O$) and post-treatment (ZVI) and it was observed that pre-modification removed 50.7–98.6% Cr, while post-modification removed 6.6–21.6% Cr [97]. Biochar prepared from pomelo peel mixed with $FeCl_3$ solution was analysed to remove Cr and phenol, and the sorbent removed Cr (24.37 mg/g) and phenol (39.32 mg/g) effectively enabled by iron oxides (Fe_2O_3, Fe^0, FeOOH, and Fe_3O_4), π–π interactions and electron donor–acceptor complex [98]. Rice straw–derived biochar was treated with $ZnCl_2$ and $FeCl_3$ to analyse removal of 17β-estradiol and Cu, and it was observed that magnetic biochar pyrolysed at 700 °C best removed 17β-estradiol (153.2 mg/g), and that pyrolysed at 300 °C best removed Cu (85.9 mg/g), with removal enabled by larger surface area, pore volume, and O-containing functional groups (–COOH, C–OH, C = O) [99]. Wheat straw–based biochar modified with α-FeOOH removed Cd (62.9 mg/g) and As (78.3 mg/g) enabled by co-precipitation and ion exchange [93]. ZVI/biochar/Ca-alginate composite removed Cr efficiently (Qe = 86.4 mg/g) along with minimal Fe release, suggestive of the resolution of problem of ZVI instability and decreased secondary pollution resulting from Fe leaching [100]. Pine wood–derived biochar ball milled with FeS_2 removed Cr more efficiently (134 mg/g) than ball milled FeS_2 (62 mg/g) and ball milled biochar (20 mg/g), with 92.25% Cr removed through reduction/precipitation and 8.75% removed via adsorption/surface complexation at equilibrium Cr concentration of 15.7 mg/L [101]. Interestingly, addition of oxalic acid promoted Cr removal from 56 to 100% in the same study. Ren et al. [102] removed phosphate using cotton stalk–derived biochar modified by ferric oxides with adsorption capacity of 0.963 mg/g and observed that coating of ferric oxides on biochar alleviated phosphate release (from 0.471 mg/g in unmodified biochar to 0.089 mg/g in modified biochar).

Al-Modified Biochar

Aluminium modification is achieved by immersing biomass in $AlCl_3$ followed by pyrolysis; stirring biochar in aqueous solution with Al electrode-based electrochemical treatment; or mixing biomass with red mud (achieved during Al production) followed by pyrolysis. Modification with Al results in an enhanced SA and selectivity, which furnishes greater Qe in composites. Additionally, there could be formation of positive charge on surface, which enables it attract anions, thereby augmenting Qe. *Mimosa pigra*-derived biochar was modified with 2 M $AlCl_3$ and observed as an effective adsorbent of NO_3^- (31.80 mg/g) and PO_4^{3-} (95.05 mg/g) [103]. Al-modified food waste biochar demonstrated high F removal (Qe = 123.4 mg/g) as high as 91.4% at wide pH range (5–11) [104].

Mn-Modified Biochar

Biochar could be modified with Mn oxides to furnish high RE, enabled by metal(loid)s entering amphoteric functional groups of MnO_x via co-precipitation, complexation, adsorption, or oxidation/reduction. For example, Mn-modified biochar is prepared by treating biomass with $MnCl_2.4H_2O$ (for manganosite crystal deposition) or $MnO_2.nH_2O$ or $KMnO_4$ (for birnessite crystal deposition) followed by pyrolysis [105, 106]. Birnessite (a mineral with oxides of Na, K, and Mn) possesses high contaminant Qe. Birnessite-loaded biochar was reported superior to manganosite-loaded biochar owing to stronger affinity of birnessite toward contaminants and enhanced synergistic reactions between cations and anions. Corn stalk–based biochar modified with $KMnO_4$ removed Cd efficiently (191.9 mg/g) enabled by greater active sites [107]. Nanomanganese oxide–modified coconut shell–derived biochar removed EDTA-Cu(II) from aqueous solutions (assisted by Fenton reaction) with removal as high as 94.7%, enabled by increased surface area, pore volume, and hydroxyl radicals [108]. FeOx-modified bone-derived biochar (pyrolysed at 450 °C) and MnOx-modified bone-derived biochar (pyrolysed at 600 °C) removed Cd (40.59 mg/g and 53.12 mg/g, respectively), Cu (56.25 mg/g and 74.78 mg/g, respectively), and Pb (178.58 mg/g and 215.03 mg/g, respectively), with greater removal in MnO-modified biochar primarily enabled by electrostatic attraction in negatively charged surface [109]. Zhou et al. [110] reported an increase in pH from 10.0 to 11.0 when corn straw–derived biochar was modified with nano-MnO_2, which eventually improved its removal efficiency (Table 2).

Bi-Modified Biochar

Bismuth is called "the wonder metal" due to easy chemical combinations (facilitated by electrons in p-orbital). Bi-modified biochar is prepared by mixing biomass with Bi_2O_3 followed by pyrolysis. Bi-mixed biomass could also be mixed with HCl (stirred at 80 °C and sonicated) followed by pyrolysis. The obtained sorbent is washed with distilled water and $NaHCO_3$. Bi-impregnation enhances SA and contaminant Qe. Bi_2O_3 inhibits tar formation, which prevents pore blockage and micropore collapse of the biochar [111]. Bi_2O_3-doped H_2O_2-modified horse manure–based biochar (carbonised at 500 °C) showed a high U(VI) removal efficiency (93.9%) with Qe = 516.5 mg/g, where removal was

enabled by precipitation, electrostatic attraction, reduction, ion exchange, and surface complexation [112].

Zn-Modified Biochar

Zinc modification makes surface of biochar positively charged, which facilitates high anion sorption. Zn modification is achieved by treating biomass/biochar with $ZnCl_2$, $Zn(NO_3)_2$, or ZnS, which loads ZnO or ZnS nanoparticles on surface and increases SA and porosity of sorbent. $ZnCl_2$-modified biochar was found superior to KOH, NaOH, $AlCl_3$, and $FeCl_3$ modifications, when considering SA, porosity, and RE [113]. ZnO-impregnated sawdust-based biochar possessed newly formed –OH groups along with large surface area (518.54 m^2/g), which helped in removal of Pb (150 mg/g) and p-nitrophenol (170 mg/g) from wastewater [114]. Glue residue–based biochar modified with $ZnCl_2$ was compared with HCl and KOH modification by Shi et al. [115], who reported that although Zn modification increased SA less than KOH modification (85.93 m^2/g, 860.45 m^2/g, and 694.03 m^2/g for HCl, KOH, and $ZnCl_2$ treatments), it showed Qe higher than HCl and KOH treatments (48 mg/g, 65 mg/g, and 80 mg/g for HCl, KOH, and $ZnCl_2$ treatments). Water hyacinth–derived biochar modified with ZnO nanoparticles removed 95% Cr (43.48 mg/g), chiefly assisted by precipitation between Cr ions and ZnO and photo-generated electrons generated by ZnO nanoparticles which reduce Cr(VI) to Cr(III) [116]. Gan et al. [117] modified sugarcane bagasse–based biochar with $ZnCl_2$ which showed pH_{zpc} (zero point charge) at 1.9 and the maximum Cr removal was observed at pH 2.0, attributed primarily to enabled by the formation of more polymerised chromium oxide species and stronger interaction between negatively charged chromate ions and positively charged functional groups of biochar at lower pH.

La-Modified Biochar

Lanthanum is a non-toxic, low-cost, and chemically stable element, which provides large number of coordination sites and augments affinity for anions. La-modified biochar is prepared by dipping biomass in $LaCl_3$ solution followed by pyrolysis. Modification could be accompanied with NaOH/ethanol treatment or the biomass could be spun in sodium alginate solution. Lanthanum modification deposits La_2O_3 on surface, which assists in contaminant removal. La-modified walnut shell–based biochar (walnut shell powder, stirred in 0.5 mol L^{-1} $LaCl_3$ solution for 2 h and pyrolysed at 400 °C) was reported as good promoter of increasing P adsorption of soil (increased Qe from 0.171 to 0.421 mg/g after amendment) where surface precipitation, ligand exchange, and electrostatic attraction were involved in adsorption [118]. La carbonate-modified and La hydroxide-modified wheat straw–based biochar were compared for P adsorption and similar Qe (64.3 and 65.0 mg/g, respectively) was obtained for both but selectivity of the latter for P (90–100%) was more than the former (73–99%) [119]. Xu et al. [120] used cattail plant–based biochar modified using La to remove phosphate (Qe = 36.06 mg/g) and observed that strong acid or alkali solutions could be effectively used for successful desorption (92% efficiency).

Mg-Modified Biochar

Magnesium is an essential element involved in synthesising chlorophyll, has low toxicity, and sorbs contaminants. It is considered a suitable cation for anion removal (e.g. As) and recovery (e.g. P). Mg-modified biochar is prepared by dipping biomass/biochar in $Mg(OH)_2$ or $MgCl_2$ and could be accompanied by acid/base or electrochemical treatment. Mg modification augments RE. Sugarcane-derived biochar coated with MgO removed Cr effectively (54.64 mg/g), and the Qe increased in H_2SO_4-assisted modified biochar (62.89 mg/g), chiefly enabled by chemical interactions between MgO and Cr [121]. Mg-modified corncob-based biochar showed 2.36–9.34 times metal sorption (Qe for Cu, Cd, and Pb is 182.7, 83.5, and 308.2 mg/g) than pristine biochar, chiefly assisted by ion exchange, complexation, cation π-bonding, and surface precipitation [122]. Mg-alginate/chitosan-modified biochar demonstrated high PO_4^{3-} sorption (Qe = 46.56 mg/g) assisted by high SA (116.2 m^2/g) [123]. Mg-modified corn-based biochar (300–600 °C pyrolysed) recovered P (Qe = 239 mg/g) from swine wastewater, which released 3.3–4.4% P during desorption in each cycle [124].

Co-Modified Biochar

Cobalt-modified biochar is prepared by treating biomass with $Co(NO_3)_2{\cdot}6H_2O$ followed by pyrolysis. The modification could be accompanied with HNO_3, HCl, ethanol, or microwave treatment to enhance biochar properties. Co modification enhances surface morphology and boosts spontaneity of contaminant sorption. Magnetic $CoFe_2O_4$-modified banana pseudostem fibre-derived biochar demonstrated high amoxicillin sorption (99.99 mg/g) over a wide pH and temperature range with dominant monolayer chemisorption, π-π stacking, H-bonding, and electrostatic interaction [125]. Wang et al. [126] modified bamboo biochar with cobalt to remove Cr and observed a decrease in pH_{zpc} from 5.8 to 3.1 after modification, primarily resulting from the neutralised or blocked protonated surface functional groups by the coated polymer layer, which eventually increased the Qe from 8.40 to 45.45 mg/g.

Ni-Modified Biochar

Nickel modified biochar is prepared by treating biomass with $NiCl_2$ followed by pyrolysis. The treatment could be accompanied with HNO_3 addition, microwave heating, or ultra-sonication [127]. Zhu et al. [128] added N-doped carbon nanotube (CNT) to biochar matrix along with Ni and KOH treatment. Ni modification increases surface properties and contaminant sorption. Diazotisation-modified Se-rich fir-based biochar was converted into NiS/NiSe/3D porous biochar (via vulcanisation and in situ competitive hydrogen reduction), which showed excellent As(III) removal performance from water (100% removal within 110 min) assisted by adsorption and photocatalysis [129]. Wang et al. [127] customised bamboo biochar with nickel to remove Pb, where modification decreased the pH_{zpc} from 5.75 to 4.72, possibly due to abundance of acidic O groups on surface, which eventually augmented the Qe from 25.0 to 142.7 mg/g after modification.

Ca-Modified Biochar

Calcium is essential for plant growth. Ca-modified biochar is prepared by immersing biomass in CaO, $CaCO_3$, and $CaCl_2$ followed by pyrolysis. The treatment could be accompanied with Fe_3O_4 or alginate modification [130, 131]. Addition of Ca helps in increasing pH and negative surface charges, which eventually augments contaminant sorption. Indian pokeweed (*Phytolacca acinosa*)-derived biochar was treated with $CaCl_2$ and Na_2CO_3 via vacuum impregnation method to deposit carbonate ions on surface, which helped remove ~ 100% Cd (154.54 mg/g), chiefly being enabled by minerals (89–98%) and Cd − π binding (2–10%) [132].

Mo-Modified Biochar

Metal removal could be enhanced by modification of surface using metal hybrids such as MoS_2. Decoration of surface with MoS_2 exposes S atoms and increases surface area and number of active sites [133]. Corn straw–derived biochar was modified with iron nitrate and ammonium tetrathiomolybdate to increase its surface area and functional groups (O-, C-, S-, and Fe-containing), and the composite removed Cd effectively (139 mg/g) > 7 times more than pristine biochar (17.8 mg/g) enabled by electrostatic attraction, Cd-π interaction, and strong Cd–S complex formation [133]. In a later study, they identified Cd–S complexation (61.7%) and Cd–O bonds (38.3%) as major players in Cd removal [134]. Sawdust-based biochar modified with ammonium tetrathiomolybdate using solvothermal reaction was analysed for Pb removal, where the S groups helped increase Qe from 32.6 mg/g in pristine biochar to 189 mg/g in MoS_2-modified biochar [135].

Multi-modified Biochar

Biochar has been modified with multiple organic and inorganic agents to improve its properties. Ca and Mg were loaded on biochar, which helped in sorbing P from biogas fermentation liquid/wastewater (Qe = 326.63 mg/g) (later recovered for fertiliser application) and the presence of CaO and MgO nanoparticles minimises negative influence of coexisting ions on sorption [136]. MgO- and Fe_2O_3-impregnated biochar removed nitrate [137], while chloride (NH_4Cl, $ZnCl_2$, and HCl)-activated biochar removed mercury [138]. Polydopamine (hydrophilic polymer with self-polymerising property, enhanced interfacial interactions with nano-ZVI, and –OH assists in dispersing nano-ZVI in adsorbent) and nano-ZVI-modified biochar removed tetracycline [139]. Corn straw–derived biochars pre-treated with $FeCl_3$ and $KMnO_4$ solutions were found to remove 91.79% Cr (118.03 mg/g) in comparison to 32.17% by pristine biochar, chiefly enabled by 3 times SA [140]. Similarly, Fe–Mn-modified *Pennisetum* straw-derived biochar efficiently removed Cd (95.23 mg/g; Qe of pristine biochar was 30.58 mg/g), primarily assisted by cation exchange, Cd-π interactions, complexation with surface functional groups, and precipitation with minerals [141]. Fe–Zn-modified *Robinia pseudoacacia* and durian shell–derived biochar (post-treated with $Fe(NO)_3.9H_2O$ and $ZnSO_4.7H_2O$) demonstrated 5 times (98.58 mg/g) and 3 times (161.14 mg/g) improved Qe when compared to pristine biochar (18.18 mg/g and 54.11 mg/g for *Robinia pseudoacacia* and durian shell–derived biochar, respectively) [142].

Moreover, several studies have combined different types of treatments (physical, chemical, or impregnation) to capture the benefits of multiple treatments for enhancing the efficacy of contaminant removal (Table 4). Zhu et al. [143] modified wheat straw–derived biochar with Bi_2O_3 mixed with HCl followed by sonication to remove Cr, P, and As with 12.2 mg/g, 16.2 mg/g, and 125 mg/g adsorption capacities. Hu et al. [144] pyrolysed *Camellia oleifera* shells with nitrates of cobalt and gadolinium, treated the biochar with 0.1 M HCl, and rinsed it alternately with ethanol and ultrapure water. The modification introduced spongy pore structure in biochar and newly generated sorption sites which enabled removal of ciprofloxacin and tetracycline accomplished with adsorption capacities of 44.44 mg/g and 119.05 mg/g, respectively. Mohan et al. [145] modified oak wood and bark with salts of Fe^{3+}/Fe^{2+} followed by NaOH treatment. While the Fe treatment introduced magnetic properties and decreased porosity, NaOH modification helped improve the porosity of the biochar. While oak bark–based biochar showed 30.2 mg/g Pb and 7.4 mg/g Cd adsorption capacity, oak wood–based biochar showed 10.13 mg/g Pb and 2.87 mg/g Cd adsorption capacity. Frišták et al. [13]

pre-treated grape seed–based biochar with HNO_3 followed by $Fe(NO_3)_3$ post-treatment. While the acid treatment augmented external, internal surfaces, and porosity, iron treatment clogged the pores and blocked the inner sphere pores but Fe impregnation also added $-NO_3$ functional groups, which eventually improved the As adsorption capacity from 5.08 to 34.91 mg/g. Various mixed combination modifications are summarised in Table 4.

Other Modifications

Microwave Pyrolysis Modification

Conventional pyrolytic methods are associated with extended production time, fast firing, outside to inside heating (energy transfer through radiation, conduction, and convection), and high synthesis cost [190]. On the contrary, microwave pyrolysis involves ~ 1/2 production cost, indirect internal heating (uniform energy transfer through dipole rotations and ionic conduction), and high energy efficiency. However, microwave pyrolysis is associated with inefficiencies such as minimal scaling-up of technology, limited penetration capacity of microwaves, and large-scale production costs [191, 192]. Nevertheless, previous investigations have analysed microwave-assisted pyrolysis, where biochar was used for removing contaminants (Table 5).

Electro Modification

Application of electric field enables efficient and homogeneous deposition of metal oxide on biochar surface by evenly depositing electrolyte and electrode (metal) ions. For electro-modification, current density of 93.96 mA/cm^2 (0–12 A and 0–100 V) is applied to a biomass using a power supply (Al electrode SA, 75.56 cm^2; electrode distance, 5 cm) in an electrolyte solution (NaCl or $MgCl_2.6H_2O$), followed by pyrolysis. Electro-modification generates strong oxidation agents (OCl^- and HOCl) or minerals on surface (like MgO, $MgAl_2O_4$, AlOOH, and Al_2O_3) from electrolyte which increases SA, microporosity, and RE [165, 193].

Ultrasonic Modification

Ultrasonic treatment could be performed before/after pyrolysis to increase porosity and hasten loading of metals or metal oxides. During ultrasonic treatment, biomass/biochar is placed in ultrasonic bath and provided 40–170 kHz of frequency and 250–1000 W of ultrasonic energy at 20–80 °C for 15–120 min [194]. The treatment is generally accompanied with other modifications, such as Ti-impregnation [195], Bi-loading [143], Fe-loading [196], ZVI-complexation [197], or Mn-impregnation [106].

Ozone Modification

Ozonation has been suggested to increase O:C ratio to augment cation exchange capacity and maintain poly-aromaticity for high biochar stability. Ozone-modified biochar is prepared by exposing biochar to ozone through ozone generator flushed with 3 L/min oxygen flow for 5 min at 25 °C [194]. Jimenez-Cordero et al. [198] exposed grape seed–derived biochar (flash pyrolysed at 800 °C) to ozone and elevated temperature (850–950 °C) in inert atmosphere to desorb the formed O-containing groups, increase the SA, and decrease the pore size (increased micro-porosity). Huff et al. [199] treated pine-derived biochar with ozone to improve its cation exchange capacity and observed a reduction in pH from 7.30 to 5.28 after 90 min ozone treatment, possibly due to the addition of acidic oxygen-functional groups on surface, while the cation exchange capacity doubled from 15.39 to 32.69 cmol/kg.

Carbonaceous Modification

Carbonaceous materials (e.g., CNT and graphene) could be utilised for biochar modification, which transfers significant properties of carbonaceous materials to biochar, decreases production cost, and proliferates their contaminant RE. Biochar is modified with graphene oxide by stirring biomass in graphene suspension for 60 min (homogenised via ultrasonic treatment) followed by pyrolysis. Graphite could be used to synthesise graphene oxide nanosheets through modified Hummers method involving H_2SO_4 and $KMnO_4$ [200]. On the other hand, CNT modification is achieved by stirring biomass in CNT suspension for 60 min (homogenised via ultrasonic treatment of 20 kHz at pulse intervals of 12 min) followed by pyrolysis. These modifications increase the contents of O-containing functional groups and SA. Carbonaceous modification could be accompanied with other treatments (e.g. sodium dodecyl-benzenesulfonate dispersion) to facilitate superior properties. Corn stalk mixed with graphene was pyrolysed at 350 °C to prepare biochar to remove Cd from aqueous solutions and it was observed that addition of graphene increased sorption capacity 1.26–2.36 times compared to pristine biochar, primarily enable by physisorption, complexation, and ion exchange [201]. Sawdust mixed with graphene oxide pyrolysed at 700 °C to fabricate the composite was used to remove Cd and it was observed as an effective sorbent of Cd (Qe = 55.68 mg/g), with adsorption following pseudo-second-order kinetics and Freundlich isotherm and column study following Admas–Bohart model [202]. Inyang et al. [203] modified hickory and bagasse bichar with CNT and sodium dodecylbenzenesulfonate to improve the Qe of lead and sulfapyridine, where the pH decreased from 7.25 to 6.74 in hickory biochar and from

Table 5 Other modifications of biochar

Feedstock; treatment	Target pollutant	Adsorption capacity or removal efficiency (RE)	Mechanism and other comments	Reference
Walnut shells; $FeCl_3$; microwave pyrolysis (20 min; 800 W)	As	1.91 mg/g	High SA (418 m^2/g); presence of iron (magnetite, hematite)	[241]
Wheat straw; microwave pyrolysis (950 °C; 15 min)	As(V) Methylene blue	25.6 mg/g 144.9 mg/g	High porosity, SA	[191]
Laminaria japonica; electro-modified ($MgCl_2.6H_2O$ electrolyte, 93.96 mA/cm^2 current density, 0–12 A, 0–100 V; Al-electrode surface area—75.56 cm^2; electrode distance—5 cm); 600 °C pyrolysed	phosphate	887 mg/g	Presence of surface minerals (like MgO, $MgAl_2O_4$, AlOOH, Al_2O_3), high SA	[193]
Corncob; ultrasonic; Ti (20 °C, 15 min); 550 °C pyrolysed; butyl titanate	Cd As	72.62 mg/g 118.06 mg/g	Complexation, ion exchange; PV (increased 5 times), reduced pore size (decreased from 9.01 to 2.42 nm)	[195]
Pine; 400 °C pyrolysed; ozone	Methylene blue	9.35 mg/g	Enhanced CEC, surface-oxygenation	[199]
Water hyacinth; graphene oxide (300 °C pyrolysed)	Cr(VI)	150.02 mg/g	Electrostatic attraction, complexation, reduction of Cr(VI) to Cr(III)	[242]
Wheat straw; graphene	Phenanthrene, Hg^{2+}	95% for phenanthrene; 80% for Hg^{2+}	π-π interactions, increased SA, functional groups –OH, C=C, O–C–O and C–O); surface sorption, complexation	[243]
Hickory chips, sugarcane bagasse; carboxyl-functionalised multi-walled CNT	Methylene blue	6.2 mg/g	Increased SA (> 350 m^2/g), PV (0.14 cc/g), thermal stability, electrostatic attraction, diffusion	[244]
Hickory, bagasse; CNT, sodium dodecyl-benzenesulfonate; 600 °C pyrolysed	Pb^{2+}, sulfapyridine	Hickory (removed 71% Pb^{2+}, 86% sulfapyridine); bagasse (removed 53% Pb^{2+}, 56% sulfapyridine)	CNT stabilisation on surface	[203]
Peanut shells; graphene	Methylene blue phenol	16.11 mg/g 46.22 mg/g	Enhanced C content (from 69.72 to 71.41%), SA (from 261 to 468.2 m^2/g), PV (from 0.09 to 0.19 mL/g); electrostatic attraction, π-π interaction	[245]
Cotton wood; graphene/pyrene (600 °C annealed)	Methylene blue	174 mg/g	π-π interactions	[246]
Eichhornia crassipes (invasive plant); chitosan	Cr^{6+}	120 mg/g	Enhanced functional groups	[204]
Bamboo, sugarcane bagasse, hickory wood, peanut hulls; chitosan	Pb^{2+}	71.5 mg/g	Amine groups assist in removal; pores filled by chitosan decreases SA, enhances contents of O, H, N	[205]
Bamboo; montmorillonite clay mineral	PO_4^{3-} NH_4^+	105.28 mg/g 12.52 mg/g	Electrostatic attraction, ionic bonding enabled PO_4^{3-} sorption; surface adsorption, high CEC assisted NH_4^+ sorption	[247]
Cassava peel; bentonite (clay); 500 °C pyrolysed	NH_4^+	100%	van der Waals force, ion exchange	[248]
Cotton wood; $ZnCl_2$, $AlCl_3$	Phosphate	410 mg/g	MgAl-layered double hydroxide (a multi-functional anionic clay)	[249]
Bamboo, bagasse, hickory chip; kaolinite, montmorillonite (600 °C pyrolysed)	Methylene blue	9–84%	electrostatic attraction, ionic exchange; increased Na, Fe, Al contents	[250]

Table 5 (continued)

Feedstock; treatment	Target pollutant	Adsorption capacity or removal efficiency (RE)	Mechanism and other comments	Reference
Pinewood; H_2O_2 (400 °C pyrolysed)	Methylene blue	7.71 mg/g	Higher CEC, oxygen-containing surface functional groups; pH decreased from 7.16 to 5.66	[251]
Cymbopogon schoenanthus; H_2O_2	Cu^{2+}	53.8 mg/g	Surface functional groups (–COOH)	[252]
Peanut hull; H_2O_2	Pb	22.82 mg/g	O-containing functional groups	[253]
	Cu	0.21 mg/g		
	Cd	1.22 mg/g		
	Ni	0.07 mg/g		
Rice husk; methanol	Tetracycline	> 95 mg/g	Esterification between biochar and carbonyl groups; O-containing groups; π-π electron interactions	[219]
Sugarcane bagasse; thioglycolic acid	As(V)	92.7%	–COOH-assisted As(V) removal; sulphur-aided As(III) sorption	[220]
	As(III)	91.45%		
Tomato (irrigated with 25 mM Mg solutions)	Phosphate	88.5%	Presence of MgO, $Mg(OH)_2$	[238]
Softwood bark, Aspen wood; microbe-colonised (biofilm)	Naphthenic acid	87%	Microbial growth; 4–7 times metal(loid) removal (As, Al, Fe)	[254]
Hard wood; *Proteobacteria*, *Clostridia*-colonised	Caffeine, ranitidine, metoprolol, carbamazepine	> 98%	adsorption, biodegradation; biofilm	[255]

**CEC* cation exchange capacity, *CNT* carbon nano tubes, *PV* pore volume, *SA* surface area

6.94 to 6.72 in bagasse biochar, possibly enabled by the addition of acidic functional groups on surface.

Chitosan Modification

Chitosan is derived from chitin and contains abundant free $–NH_2$, –OH, and hydrogen bonds (between the main chains in secondary structure), which provides ion exchange, chelation, and contaminant sorption ability. Chitosan-modified biochar is prepared by stirring biochar in 2% acetic acid solution containing chitosan for 30 min at 40 °C followed by addition of glutaraldehyde and suspension into NaOH solution for 1–12 h [204, 205]. The treatment could be accompanied with addition of ZVI to enhance its RE [148]. Walnut shell–derived biochars were modified with beta-cyclodextrin–chitosan to remove Cr from aqueous solutions, and an RE of 93% was achieved (Qe = 206 mg/g), primarily enabled by electrostatic attraction of $HCrO_4^-$ and $Cr_2O_7^{2-}$ to positively charged surface and complexation with $–NH_2$ and –OH functional groups [206]. Rice straw–derived biochar (450 °C pyrolysed) was modified with chitosan and pyromellitic dianhydride to increase amide and carboxyl groups, which could strongly interact with contaminants via electrostatic attraction, ion exchange, and complexation [207]. Modification improved the RE by ~ 10% with Qe of 8.62 mg/g, 25.78 mg/g, and 71.40 mg/g for Pb, Cd, and Cu, respectively. Chitosan-combined magnetic Loofah sponge-based biochar removed Cr (30.14 mg/g) and Cu (54.68 mg/g) efficiently, mostly assisted by ion exchange and surface complexation, despite the decrease in SA (from 337.35 to 96.91 m^2/g) [208].

Clay/Silt/Silica Modification

Biochars could be loaded with clay minerals, such as bentonite, montmorillonite, or kaolinite, to modify its composition and properties to increase sorption of oxyanions, like PO_4^{3-}, and polyatomic cations, like NH_4^+. Typically, biomass is mixed with a suspension of ultrasonicated (form homogenisation) clay minerals, stirred for 60 min and pyrolysed to obtain amorphous biochar with crystalline clay minerals. Additionally, higher pyrolytic temperatures evaporate water molecules from clay minerals, which reduces pore volume (PV) (and pore diameter) [17]. The treatment is enhanced by activation under CO_2 flow for greater microporosity. Rawal et al. [209] pyrolysed bamboo biomass, pre-treated with iron sulphate-clay mixture, at 250–550 °C to obtain clay-modified biochar with enhanced PV and mineral infusion into pores (high content of S, Fe, and Al). Yao et al. [210] reported > 15% enhanced green pepper yield, > 1 0% increased vitamin C content, and ~ 1/3rd decreased nitrate content after amendment with wheat straw–derived biochar (pre-treated with urea, minerals, and H_3PO_4) compared to conventional fertilisers. Oiltea camellia shell–derived biochar modified with silicon was observed to possess augmented surface area (45–112%) and porosity (5–12%) and Cd removal was enabled by complexation with –COOH and C–Si–O groups, surface precipitation ($CdCO_3$, $CdSiO_3$, or Cd_2SiO_4), coordination with π electrons (C = C), and ion exchange with Na^+ [211]. Rosin-based bentonite-coated Fe_2O_3 nanoparticle-supported biochar removed 95% Cr(VI) within 1 min (81.7 mg/g) mainly due to the key role played by α-Fe_2O_3 nanoparticles [212]. Cigarette factory waste–derived biochar modified with bentonite and calcite minerals removed Pb efficiently (99%), with bentonite and calcite catalysing changes in yield, carbonisation, minerals, functional groups, texture, and pH [213]. Siltstone-nanomagnetite-modified *Eleocharis dulcis*–derived biochar demonstrated high Cr Qe (35.57 mg/g), assisted by electrostatic attraction [214]. Montmorillonite-modified wheat straw–based biochar showed high norfloxacin Qe (increased from 10.58 to 25.53 mg/g after modification), enabled by pore filling, H-bonding, and electrostatic interaction [215]. They also stated that presence of humic acid and Cu^{2+} could reduce norfloxacin sorption due to competitive adsorption and pore blockage. Montmorillonite-modified corncob-based biochar removed Pb (139.78 mg/g) and atenolol efficiently (86.86 mg/g) enabled by hydroxyl O atom acting as a possible reaction site and amino N and amide O atom providing lone pair of electrons, which generates H-bond or strong electrostatic interactions with surface functional groups [216].

H_2O_2 Modification

Hydrogen peroxide (H_2O_2) is a clean and less-expensive product proposed to modify biochar for high sorption. Typically, H_2O_2-modified biochar is prepared by placing biochar in H_2O_2 solutions (1–30%) and stirred for 120–180 min followed by filtration, washing, and drying. H_2O_2 modification was compared with H_2SO_4, HNO_3, and KOH modifications, where H_2SO_4 and HNO_3 treatments caused porosity loss and heterogeneous micropore distribution, while H_2O_2 and KOH treatments enhanced homogenous micropore distribution, micro-PV, and SA. All the treatments enhanced acidic surface functional groups, which enabled biochars (rice straw derived) in removing contaminants like methylene blue, phenol, and iodine [56, 217]. Wongrod et al. [45] reported decreased As removal after H_2O_2 and KOH modification of biochar (while H_2O_2 oxidised organic content, KOH dissolved ash). Pig manure–derived biochar was oxidised using H_2O_2 (oxidation occurred at C = C bonds) and thiolated using 3-mercaptopropyltrimethoxysilane (sulphur content increased to 4.43%), where sorption capacity of biochars augmented by 2.5–4.2 times for Cd and Pb with increase in pyrolysis temperature from 300 to 700 °C [218]. Metal

removal was enabled by cation exchange, complexation with functional groups, cation-π EDA interaction, and precipitation with minerals.

Organic Solvent/Compound Modification

Biochar could be modified with organic solvents such as methanol and thioglycolic acid to increase the content of surface functional groups (especially carboxyl and carbonyl groups). However, the volatile nature and high costs associated with the organic solvents limit their real-time large-scale applicability for biochar modification. Previously, organic solvent-modified biochar was used to remove contaminants (Table 5) [219, 220]. Organic compounds like thiourea, polyaniline, and poly(vinyl alcohol) (PVA) have been used to modify biochar. Swine sludge–derived biochar was pre-treated with NaOH and HNO_3 and modified with thiourea to augment C–O, C = O, C–S, C = S, and RSO_3^- groups, which enabled high Pb removal (Qe = 143.13 mg/g) [221]. Rice husk– and *Eucalyptus* saw dust–based biochar was modified with polyaniline to graft NH_2 groups of polyaniline directly on surface, where an increase in SA (38.7–41.3 m^2/g) and Cr removal (72.31–81.43%) was observed [222]. Rice straw–derived biochar was aminated with poly(vinyl alcohol), epichlorohydrin, and diethylenetriamine to augment surface functional groups (such as –OH) and Cr(VI) removal (Qe = 140.39 mg/g) [223]. $KMnO_4$-modified corncob-based biochar was entrapped/immobilised in poly(vinyl alcohol)/sodium alginate hydrogel beads to study Cu removal and an increase in Qe was observed (23.70 mg/g in pristine biochar; 87.07 mg/g after modification), probably due to inner-sphere complexation (Cu–O, Mn–O–Cu bonds) [224]. 3-aminopropyltriethoxysilane and polyamidoamine dendrimer-modified magnetic rice straw–derived biochar removed Cu efficiently (251.81 mg/g) mainly due to electrostatic attraction and bridging influences with $–NH_2$ groups, despite the decrease in SA [225].

Nitrogen Modification

Biochar is modified with N by recapturing N from wastewater (polar functional groups enable sorption in low temperature–synthesised biochars; high SA enables sorption in high temperature–pyrolysed biochars). Biochars could recover nitrates and ammonium from human urine present in wastewater treatment plants [226]. Polyethylenimine and methanol were used to augment N- and O-containing groups (primarily amino groups) in rice husk–derived biochar to sorb Cr (Qe = 435.7 mg/g) [227]. Stillage-derived biochar was loaded with N-containing phosphates (urea phosphate, ammonia polyphosphate, and ammonia phosphate) to augment its porosity (0.464 cm^3/g) and SA (798 m^2/g), which sorbed toluene effectively (Qe = 496.2 mg/g) [228]. Saw dust–derived biochar was treated with H_2SO_4, HNO_3, NH_4OH, $Na_2S_2O_4$, and glacial CH_3COOH to furnish amino groups, which helps sorb Cu^{2+} (Qe = 16.11 mg/g) [229]. Rice straw–derived biochar was modified with iron and (3-aminopropyl)-triethoxysilane to enhance Fe and NH_2 radicals to augment Cr (100.59 mg/g) and Zn removal (83.92 mg/g) [230]. Waste-derived biochar (municipal waste, oak wood, anaerobic digestate press cake, and greenhouse waste; pyrolysed at 450–650 °C) sorbed ammonium (Qe = 146.4 mg/g) and phosphate (Qe = 37.1 mg/g) [231]. Takaya et al. [231] also reported minimal desorption of ammonium (5.1 mg/g) and phosphate (8.5 mg/g), which could enable its usability as slow release soil amendments.

Sulphur Modification

Sulphur modified biochar could be prepared by sorbing H_2S produced during anaerobic digestion of biomass for bioenergy generation. Dairy manure–derived biochar adsorbed H_2S generated during anaerobic digestion of organic waste and obtained S-modified biochar (36.5% S) [232]. S modification could also be achieved by surface modification with reagents like thiols, CS_2, or SO_2 [233, 234]. S-modified biochars immobilise Hg in soils, primarily enabled by the strong affinity of S for Hg. Rice husk–derived biochar modified with S (13.04% S) minimised Hg contamination by ~ 73% (Qe = 67.11 mg/g) primarily by forming HgS [235]. Na_2S-modification of corn straw–based biochar enhanced Hg^{2+} sorption by 76.95% and atrazine sorption by 38.66% [76]. Oilseed rape straw–derived biochar (with enhanced S) immobilised methyl-Hg by complexation and reduced methyl-Hg accumulation in rice grains [236]. Corncob biochar modified with Na_2S showed best Ni removal (15.40 mg/g), SA (195.64 m^2/g), and PV (0.2340 cm^3/g) among modified crayfish shell, cotton stalks, corncob, and peanut shell-based biochars, chiefly enabled by ion exchange [237].

Living Feedstock Modification

There was a unique and interesting study where plants were irrigated with metal-rich water to enhance the contents of essential nutrients in plants which could boost its yield. Yao et al. [238] irrigated tomato plants with 25 mM Mg solutions to obtain Mg-enriched tomato tissues. Later, it was pyrolysed to produce biochar, where pyrolysis augmented Mg concentrations in the sorbent (8.8% Mg). The presence of MgO and $Mg(OH)_2$ provided greater removal of phosphate (88.5%).

Microbe Modification

The property of high SA enables biochar in facilitating the growth and colonisation of microorganisms on its surface. The colonised microbes develop a biofilm on surface via secretion of adhesives (polymers), which facilitates stronger viability (due to protection provided by biofilm). The inoculation and colonisation of microbes aids in degrading organic contaminants and biosorbing metals [17]. Microorganism-colonised (*Streptomyces violarus* strain SBP1) H_2O_2-modified wood waste–derived biochar effectively removed ~ 74.8% Mn(II) and oxidised it into lesser toxic Mn(III) and Mn(IV) [239]. Since biofilm-associated biochar could assist in removal of contaminants, it was suggested for application as filters and treatment of polluted water, wastewater, and soils [240].

Mechanistic Insights into Contaminant Removal

Different models have been proposed to identify processes involved in adsorption, where adsorption capacity of contaminants is plotted against initial concentration, contact time, and temperature to diagnose the best fitting isotherm, kinetic, and thermodynamic model. Langmuir and Freundlich are the most used adsorption isotherm models [256–258], while Lagergren pseudo-1st order, pseudo-2nd order, intra-particle diffusion, and Elovich are the most used adsorption kinetic models [259–261]. Thermodynamic parameters like entropy, enthalpy, and Gibbs free energy are calculated by plotting adsorption capacity versus temperature [262]. Previous studies have proposed the following mechanisms as chiefly involved in removal of contaminants (Fig. 2): (i) precipitation/co-precipitation, (ii) complexation (coordination, surface complexation), (iii) ion exchange (anion and cation exchange), (iv) physical adsorption, (v) specific adsorption (including chemical process), (vi) electrostatic interaction/attraction/attachment, (vii) reduction, (viii) π-bond interaction, and (ix) micro-electrolysis reaction [263]. For example, Cr (which exists as Cr(VI) and Cr(III), with + 6 state being more toxic) removal primarily involved electrostatic interaction, complexation, reduction from Cr(VI) to Cr(III) through surface functional groups such as –OH and –COOH and ion exchange with Al^{3+}, H^+, and Zn^{2+} [222, 264, 265]. Cd (existing as Cd(II) and hydrxo-complex) removal chiefly incorporates complexation with functional groups (O-, C-, S-, and Fe-containing) and ion exchange with Ca^{2+}, Na^+, and K^+, apart from physical adsorption and electrostatic attraction [133, 141, 201, 265]. As (existing predominantly in $H_2AsO_4^-$ and $HAsO_4^{2-}$ at 3–6 pH and AsO_4^{3-} at alkaline pH) removal mainly involves electrostatic interactions (with –OH and –COOH groups on surface) and complexation/precipitation (with metals and metal oxides on surface), apart from redox transformation, ion exchange, and H-bonding [266]. Pb (primarily prevalent as Pb(II)) removal

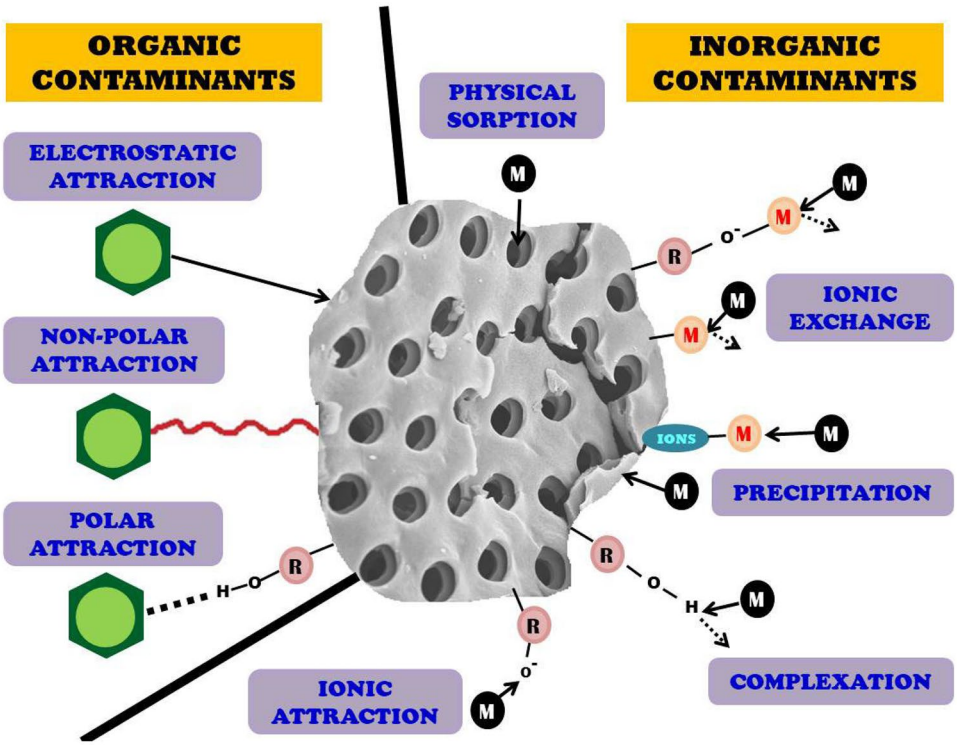

Fig. 2 Contaminant removal by modified biochar

involves complexation with C–O, –OH, –SH, and C–S functional groups (mainly inner-sphere surface complexation), chemisorption with ion-exchange groups (R–SH and $–RSO^{3-}$) and coordination groups (–COO, –C = S, –C–NH_2) [135, 221]. Cu (occurring as Cu(I) and Cu(II), with + 2 being more harmful) removal incorporates complexation with surface functional groups (such as –COOH, –OH, and –NH_2) [229]. Removal of Pb(II) and Cd(II) involved ion exchange, specific adsorption (Pb/Cd–O or hydroxyl binding), and electrostatic attachment [170]. When competitive adsorption of Pb(II), Cd(II), and Cu(II) was investigated, differential role of functional groups was observed, with N–C = O group majorly involved in Pb(II) removal, C = C and N-containing groups involved in Cd(II) removal, and carbonyl and N-containing groups involved in Cu(II) removal [207].

pH is a crucial factor influencing the removal of contaminants by modified biochars. For example, heavy-metal ions precipitate in alkaline environment, thereby affecting the Qe of modified biochars. The contaminants form complexes with OH^- or H^+ under alkaline or acidic environments, which affect the RE of modified biochars [263]. Changes in surface functionality also affect the acidic/alkaline properties of modified biochars, eventually affecting contaminant removal. pH at zero point charge (pH_{zpc}) affects the surface charge of modified biochars by changing the protonation effect of surface functional groups of modified biochars in acidic conditions. While a pH lower than pH_{zpc} makes the surface of modified biochars positively charged and attracts anionic contaminants, a pH higher than pH_{zpc} makes the surface negatively charged, augmenting the electrostatic attraction of cationic contaminants. Solution pH is another factor governing the removal of contaminants by modified biochars. For example, an increase in solution pH from 2 to 8 augmented the removal of Cd by $MgCl_2$-modified biochar from 47.17 to 98.30% [267]. In general, a decrease in pH of biochar after modification is observed. While Huff et al. [199] observed a reduction in pH (from 7.30 to 5.28) after ozonation, Wang et al. [126] and Wang et al. [127] reported a reduction in pH_{zpc} of biochar after modification with nickel (from 5.75 to 4.72) and cobalt (from 5.8 to 3.1), respectively, which increased Qe from 25.0 to 142.7 mg/g and from 8.40 to 45.45 mg/g, respectively. However, an increase in pH has also been reported after modification, like an increase from 10 to 11 after modification with nano-MnO_2 eventually improving removal efficiency as reported by Zhou et al. [110].

Surface properties of modified biochar (SA, charge, and functionality) are involved in removal of emerging organic contaminants [18]. Chemical modification generates abundant adsorption sites, making the surface favourable for surface precipitation, surface complexation, and electrostatic attraction, while physical modification influences SA and microporosity, which affects mechanisms like intra-particle diffusion and pore filling [268]. H_3PO_4-modified pig manure–derived biochar removed tetracycline primarily through π-π electron donor–acceptor interaction and hydrogen bonding [269]. Chitosan and Fe/S-modified sludge-based biochar removed tetracycline primarily using π-π stacking, hydrogen bonding, silicate bond interaction, and pore filling, but also involved chelation and ion exchange, which rarely occurs during adsorption of organic contaminants [270]. KOH-treated potato stem and leaf-derived biochar adsorbed ciprofloxacin via π-π interactions, electrostatic interaction, and hydrogen bonding [271]. Magnetised pine sawdust–based biochar adsorbed ethinyl estradiol and sulphamethoxazole primarily through π-π electron donor–acceptor and hydrophobic interaction [272]. Magnetic bagasse biochar nanoparticles removed 17β-estradiol chiefly via simultaneous hydrophobic interactions (dominating at lower pyrolysis temperatures) and π-π electron donor–acceptor interactions (dominating at higher pyrolysis temperatures) [273]. Ca- and Fe–Mn-modified litchi-derived biochars were suggested to effectively control estrone/estrogen in water and soil environments, where immobilisation was primarily achieved through hydrogen bonding interaction [274]. Magnetic Fe2O3–modified banana peel–based biochar effectively degraded bisphenol-A (completely removed within 20 min), without pH adjustment, through hydrogen bonding and involvement of surface functionality [275]. Bamboo-derived biochar supported $CuZnFe_2O_4$ composite removed bisphenol-A and sulphamethoxazole through hydrogen bond interaction, hydrophobicity, and π-π interactions [276]. Cotton straw–based biochar removed sulphonamide primarily via van der Waals and hydrophobicity [277]. Tylosin removal using novel goethite biochar was assisted by hydrophobic, π-π electron donor–acceptor electrostatic, cation exchange, and H-bonding interactions, with best fitting of Henry and Freundlich models [278]. KOH-treated wild plum–derived biochar modified with microwave treatment (700 W for 12 min) removed naproxen efficiently (73.14 mg/g) with maximum assistance from electrostatic attraction between positively charged –OH groups on surface and negatively charged naproxen [279]. NaOH-activated alfalfa-derived biochar superiorly removed tetracycline from water (302.37 mg/g), with prime involvement of chemisorption interaction and intra-particle diffusion [78]. MgAl-double lamellar hydroxides/bovine bone–based biochar composite completely removed caffeine from water within 20 min (26.22 mg/g), with best fitting of Redlich–Peterson, indicating that both monolayer and multilayer adsorptions are involved in the removal of caffeine [280]. Overall, electrostatic interactions, cation exchange, surface complexation, hydrogen bonding, and non-specific van der Waals interactions are involved in removal of organic contaminants [281].

Modified Biochar and Ageing

Biochars undergo ageing when applied in the environment, primarily under the influence of natural forces including temperature-induced freeze–thaw cycles, rainfall-induced wetting–drying cycles, sunlight-induced photochemical degradation, and mild forms of oxidation (arising from microorganisms, root exudates, or atmospheric oxygen) [282]. Ageing affects physico-chemical properties like aromaticity, elemental composition, surface morphology, and surface area, which could either increase or decrease removal of organic/inorganic contaminants by biochar. In general, chemically/biologically oxidised biochar removes pronounced amounts of inorganic contaminants, aided by higher surface complexation with O-containing functional groups and retained ash content, which furnishes contaminant co-precipitation. On the contrary, physically aged biochars demonstrate diminished contaminant removal because of lower mineral content and O-containing groups, which minimises complexation and co-precipitation. With respect to ageing, contrasting results of decrease in contaminant removal (Cu and Pb removal decreased due to wet-dry ageing, as reported by Shen et al. [283]) and increase in contaminant remediation (Cd and Pb removal increased by KOH-modified biochar, reported by Wang et al. [284]) after application of biochar has been reported previously. Such contrasting reports could be emanating from dissolved organic matter–induced contaminant mobilisation or O-containing group-supported contaminant immobilisation [285, 286]. Biochar ageing favours microbial degradation of organic contaminants, where biochar acts as electron shuttle between organic contaminants and microorganisms colonised on external and internal surface and with progressive ageing, enhanced O-containing groups favour electron shuttle effect.

Huang et al. [287] prepared Ce/Mn-modified wheat straw biochar to remove As(V), where the team assessed the influence of three different ageing processes (natural, freeze–thaw, and dry–wet cycles) on the adsorption performance of modified biochar. Interestingly, freeze–thaw ageing increased the SA of modified biochar (214.98 m^2/g) more than the other two ageing processes. However, pH and C contents reduced after ageing, but contents of H and O increased after ageing. Qe augmented by 16.2% and 10.6% for freeze–thaw and dry–wet ageing treatments, respectively. Freeze–thaw and dry–wet ageing processes also activated Ce/Mn oxides in augmenting $Mn^{2+/3+}$ and Ce generation, eventually increasing $CeAsO_4$ precipitation and Ce/Mn–O–As complexation. In an interesting study, Wang et al. [288] prepared aged biochars by treating corn straw–derived biochar with 20% H_2O_2 at 1:20 (w/v) ratio for 24 h. The team observed a decrease in Cd and Pb RE attributable to a reduction in mineral precipitation and cation exchange mechanism. In another study, Cui et al. [289] simulated Fenton-like chemical ageing by oxidising peanut and bush biochar with citric acid/Fe_2O_3 and citric acid/$FeCl_3$. The team observed that ageing improved surface properties, surface functionality, and elemental content in biochars, which increased 2,4,6-trichlorophenol removal by 1–11% and 7–38% in aged bush and peanut shell biochar, respectively. The contrasting results trigger the need for performing extensive studies to examine the adsorption/degradation performance of modified biochars with respect to ageing. It is also noteworthy that production temperature could affect the adsorption performance of ageing biochar [290]. While high temperature biochars demonstrate lower Qe when exposed to acid rain leaching or oxidation (which remove inorganic alkaline elements and minimises pH), low temperature biochars display an increase in Qe, assisted by augmented O-containing groups (which promotes ion exchange and surface complexation). A major condensed aromatic carbon portion of biochars remain very stable, the labile portion still remains biodegradable [291].

Theoretically, biochars could immobilise contaminants for a very long term, but Shen et al. [283] reported metal immobilisation for a short term and mobilisation with an accelerated ageing simulated by a wet-dry-ageing experiment (for example, metals such as Cd, Cu, Pb, Ni, and Zn). Therefore, utilisation of biochar for immobilising contaminants in soils could pose long-term risks and might necessitate further enquiry for safer application. Martin et al. [292] compared un-aged biochars to 32-month-aged biochars and observed that removal of contaminants like diuron and atrazine minimised significantly in the latter by 47–68%. Similarly, Ren et al. [293] suggested that adsorption performance of biochar amended soils (for contaminants like atrazine and phenanthrene) reduced to levels of untreated soils after 30 months of application. However, Jones et al. [294] reported that 2-year ageing did not affect the RE of contaminants like simazine. A 3-year experiment by Li et al. [295] observed that hardwood-derived biochar minimised Cu and Cd concentrations by 63.8% and 57.9%, respectively in first year in soil, but the biochars increased mobilisation in the following years. On the contrary, corn straw–derived biochar minimised metal concentrations steadily throughout the experiment. Such a variation in results was attributed to the differences in lignin content. These observations signify that it is crucial to choose the appropriate kinds of feedstock to minimise the bio-availability and mobility of contaminants stably for longer periods in contaminated environments.

Feasibility and Limitations of Biochar Modification

The feasibility of modified biochars is dependent on a number of factors inclusive of the biochar properties, the costs of fabrication, the risks associated with their application, and the viability of its scalability (from lab scale to industrial scale). The physico-chemical properties of the modified biochars depend on the type of feedstock used, treatment temperature, and the modification method. An improved understanding of the properties would enable a better utilisation of the fabricated adsorbents for various applications including removal of contaminants. The calculation of costs of fabrication is complicated and depends again on the feedstock, treatment temperature, and the modifying agent. Waste biomasses, which are typically free, could be used to minimise the costs of production. However, assessment of costs becomes difficult, when factors such as treatment cost, transportation tariffs, labour charges, energy consummation, and operating and maintenance costs are included in the cost calculation, as these are typically the most crucial components of biochar preparation on a large scale [2]. Interestingly, Inyang and Dickenson [296] suggested that on an average unmodified biochar cost ~ 1/6th of the production costs of activated carbon (~ $1500/ton). Such a large difference in production costs could be used to advantage for the fabrication of modified biochars, where only an additional expense of the modifying agent or treatment condition would need to be incorporated. Most of the studies reviewed focussed on batch studies using modified biochars for contaminant removal, while the actual performance of the adsorbent needs to be examined with column/continuous setups incorporating real-time contaminated soil/water in addition to subjecting the adsorbent to multiple sorption-regeneration cycles. Additionally, recovery of the adsorbent and its stability after real-time application for removal of contaminants would be crucial in enhancing the feasibility of the fabricated adsorbent. Recovery and regeneration of adsorbent would critically depend on the mechanisms involved in contaminant sorption, where weaker binding of contaminant (via physisorption) to adsorbent would amplify the regeneration and reusability of adsorbent, when compared to a stronger bonding (involving chemisorption) between adsorbent and contaminants [2].

It must also be observed that different studies comparing different biochar modifications have reported a superior performance of one or the other biochar modification, which on the first instance could intricately confuse the research team in selecting the appropriate modification method. For example, while Wang et al. [50] reported alkaline modification to be superior to acid modification, Zhang et al. [60] reported the contrary superiority of acid modification for contaminant removal. However, Liu et al. [297] suggested that acidic modifications persist with issues of non-recyclability, higher pollution, and larger consumption of activation energy, while alkaline modifications are associated with advantages of higher biochar yield, lower activation temperature, and controllable void structure, which could be suggestive of the preferability of alkaline modifications, also re-affirmed by Lima et al. [20] and Hussain et al. [66]. It makes it crucial for the future research teams to compare the different modification methods for a better understanding of the feasibility and the limitations of its applications, especially removal of contaminants. Modifications such as steam and gas treatment, alkaline treatment, and carbonaceous modification improve the surface area and porosity of adsorbent. However, steam, gas, and carbon modification are associated with high costs, while alkaline treatments are much less costly and could favour their usability. Additionally, physical modifications consume huge amounts of energy, which increases the production costs and makes the fabrication non-greener. Different modifications influence the elemental composition of biochars differently, which affects the basic or hydrophilic nature of biochar [16]. For example, nitrogen-to-carbon ratio regulates basic nature of biochar, while oxygen-to-carbon ratio dictates the hydrophilic nature of biochar. Alkaline treatments when compared to acidic treatments increase basicity and aromaticity of biochar and decreased the hydrophilic nature by altering the carbon, oxygen, and nitrogen contents of biochar. Treatments involving alkaline and oxidising agents augment oxygen-containing functional groups on surface. While alkaline treatments augment hydroxyl and carboxylic groups, oxidising treatments increase carboxylic groups. However, it is also important that after modification, the acid/alkali solutions might need further treatment, which could eventually complicate the fabrication of biochar. In due course, acid/alkali solutions could be treated by neutralising it with alkali/acid solutions. Also, the costs of modifying agents need to be kept into perspective, which could limit its applicability. Nonetheless, cyclic utilisation of modifying agents could minimise the costs of fabrication. When compared to other treatments, metal impregnation enhances the active adsorption sites the most, thereby supporting the removal of contaminants the most. Still, previous reports have suggested leakage of metal ions from the adsorbent, which could influence the stability of modified biochars [19]. By and large, the selection of modification methods depends on the costs of fabrication or the feasibility of follow-up treatments required during modification.

Future Perspectives

- With evolving biochar treatment/modification methods, optimisation of feedstock variation, production condition, and modification route have become inevitable. Studies have been limited to laboratory setups and need proliferation for pilot-scale industrial and commercial application, inclusive of actual contaminated soil and water for determining real-time efficacy.
- Fewer studies have focussed on the removal of contaminants from simulated/industrial wastewater using modified biochars. Further, application of modified biochars for contaminant removal from large-scale industrial wastewater has not been reported. Lesser investigative analysis has been performed on mixed multi-contaminant systems and identification of the probable involved mechanisms could be crucial in the future studies.
- There is a need to investigate the stability of modified biochar composites. Long-term experiments would be needed to examine the bonding strength of composite and achieve a composite with long lifetime and high adsorption capacity under changing climatic scenarios [298, 299].
- Contrasting results were obtained in studies performed on the impact of ageing on adsorption performance of biochars. Moreover, minimal studies have analysed the adsorption behaviour of modified biochars exposed to ageing. Such a scenario triggers the need for performing extensive studies to examine the adsorption/degradation performance of ageing-modified biochars.
- Life cycle assessment of modified biochars should be performed to compare its applicability with sorbents, presently used at industrial setups, considering factors like contaminant RE, biochar stability, biochar reuse, fabrication cost (production and modification), and real-time applicability (transportation, labour involved, and maintenance).

Conclusions

Physical and chemical modification of biochar could enhance the contents of O-containing functional moieties and SA, which eventually assists in sorption of organic and inorganic contaminants. In general, acidic modifications enhance surface functional groups and cation exchange capacity, which promotes ion exchange and sorption of cationic and anionic contaminants. Alkaline modifications facilitate high aromaticity, apart from improving hydrophobicity and contaminant RE. Sorption of oxyanions could be escalated by metal impregnation in biochar. Metal-impregnated biochars sorb contaminants effectively with mechanisms involving chemisorption, electrostatic attraction, and complexation. Biochar could be facilitated with magnetic properties (via Fe modification) to ease its recovery. Pb could be effectively removed by metal/metal oxide-impregnated biochars because of the formation of stable inner sphere complexes. Cd could be better removed by Mn-modified or alkali-modified biochars because of the facilitation of surface basicity that favours electrostatic attraction with cations. Cu could be preferably removed by nitrogen-doped or metal/metal oxide-modified biochars because of the formation of N–Cu complexes. Cr could be efficiently removed by Fe-modified biochar because of the mild reduction reactivity possessed by ZVI, while Cr(VI) is reduced to Cr(III) by oxidising Fe to Fe(III) and formation of Cr(III) hydroxides. Hg could be removed by S-impregnated biochar, as it enables HgS precipitate formation apart from O-containing functional groups involvement in Hg sorption. As could be preferably removed by metal-modified biochars, primarily enabled by electrostatic attraction and formation of complexes with metals. Modified biochars (especially metal oxide and metal salt modification) show high removal of organic contaminants enabled by electrostatic interactions, cation exchange, surface complexation, hydrogen bonding, and van der Waals interactions. In view of contaminant removal and waste management, production of modified biochars from diverse agro-ecological waste could be critical for planet survivability. However, it would be beneficial to perform reality check of contaminant removal using modified and tailor-made biochars with real-time wastewaters and actual contaminated soils along with identifying routes of scaling-up the fabrication of low cost environment-friendly modified biochars and determining the influence of ageing on the stability and adsorption performance of the modified biochars.

Author Contributions Abhishek Kumar: conceptualisation, data curation, visualisation, and writing—original draft preparation; Tanushree Bhattacharya: supervision, visualisation, conceptualisation, and writing—review and editing; Wasim Akram Shaikh: writing—review and editing; Sukalyan Chakraborty: visualisation and writing—review and editing; Dibyendu Sarkar: visualisation and writing—review and editing; Jayanta Kumar Biswas: visualisation and writing—review and editing.

Funding Abhishek Kumar is grateful to the University Grants Commission, New Delhi, for giving NET-JRF Fellowship [Ref. No.- 3635/(OBC)(NET-DEC.2015)].

Data Availability All data generated or analysed during this study are included in this published article.

Code Availability Not applicable.

Compliance with Ethical Standards

Ethics Approval Not applicable.

Consent to Participate Not applicable.

Consent for Publication Not applicable.

Conflict of Interest The authors declare that they have no known competing financial interests or personal relationships that could have appeared to influence the work reported in this paper.

Human and Animal Rights and Informed Consent This article does not contain any studies with human or animal subjects performed by any of the authors.

References

1. Benis KZ, Motalebi Damuchali A, McPhedran KN, Soltan J. Treatment of aqueous arsenic – a review of biosorbent preparation methods. J Environ Manage. 2020;273.
2. Benis KZ, Damuchali AM, Soltan J, McPhedran KN. Treatment of aqueous arsenic – a review of biochar modification methods. Sci Total Environ. 2020;739:139750. Available from: https://doi.org/10.1016/j.scitotenv.2019.135577
3. Shaikh WA, Alam MAOA, Alam MAOA, Chakraborty S, Owens G, Bhattacharya T, et al. Enhanced aqueous phase arsenic removal by a biochar based iron nanocomposite. Environ Technol Innov. 2020;19:100936. Available from: http://www.sciencedirect.com/science/article/pii/S2352186420301577
4. Alam MAOA, Shaikh WA, Alam MAOA, Bhattacharya T, Chakraborty S, Show B, et al. Adsorption of As (III) and As (V) from aqueous solution by modified Cassia fistula (golden shower) biochar. Appl Water Sci. Springer International Publishing; 2018;8:1–14. Available from: https://doi.org/10.1007/s13201-018-0839-y
5. Shaikh WA, Islam RU, Chakraborty S. Stable silver nanoparticle doped mesoporous biochar-based nanocomposite for efficient removal of toxic dyes. J Environ Chem Eng. 2021;9:104982. Available from: https://www.sciencedirect.com/science/article/pii/S2213343720313312
6. Kumar A, Bhattacharya T, Shaikh WA, Roy A, Mukherjee S, Kumar M. Performance evaluation of crop residue and kitchen waste-derived biochar for eco-efficient removal of arsenic from soils of the Indo-Gangetic plain: a step towards sustainable pollution management. Environ Res. 2021;200:111758. Available from: https://www.sciencedirect.com/science/article/pii/S0013935121010525
7. Kumar A, Bhattacharya T. Biochar: a sustainable solution. Environ Dev Sustain. 2021;23:6642–80. Available from: https://doi.org/10.1007/s10668-020-00970-0
8. Kumar A, Bhattacharya T. Removal of arsenic by wheat straw biochar from soil. Bull Environ Contam Toxicol. 2022;108:415–22.
9. Kumar A, Bhattacharya T, Mozammil Hasnain SM, Kumar Nayak A, Hasnain MS. Applications of biomass-derived materials for energy production, conversion, and storage. Mater Sci Energy Technol. 2020;3:905–20. Available from: http://www.sciencedirect.com/science/article/pii/S2589299120300665
10. Shaikh WA, Kumar A, Chakraborty S, Islam RU, Bhattacharya T, Biswas JK. Biochar-based nanocomposite from waste tea leaf for toxic dye removal: from facile fabrication to functional fitness. Chemosphere. 2022;291: 132788.
11. Shaikh WA, Kumar A, Chakraborty S, Naushad M, Islam RU, Bhattacharta T, et al. Removal of toxic dye from dye-laden wastewater using a new nanocomposite material: isotherm, kinetics and adsorption mechanism. Chemosphere. 2022;136413. Available from: https://www.sciencedirect.com/science/article/pii/S004565352202906X
12. Kumar A, Bhattacharya T, Shaikh WA, Chakraborty S, Owens G, Naushad M. Valorization of fruit waste-based biochar for arsenic removal in soils. Environ Res. 2022;213:113710. Available from: https://www.sciencedirect.com/science/article/pii/S0013935122010374
13. Frišták V, Moreno-Jimenéz E, Fresno T, Diaz E. Effect of physical and chemical activation on arsenic sorption separation by grape seeds-derived biochar. Separations. 2018;5.
14. Premarathna KSD, Rajapaksha AU, Sarkar B, Kwon EE, Bhatnagar A, Ok YS, et al. Biochar-based engineered composites for sorptive decontamination of water: a review. Chem Eng J. 2019;372:536–50. Available from: https://www.sciencedirect.com/science/article/pii/S1385894719308757
15. Kumar A, Nagar S, Anand S. Nanotechnology for sustainable crop production: recent development and strategies. Adv Sci Technol Innov. 2021. p. 31–47.
16. Ahmed MB, Zhou JL, Ngo HH, Guo W, Chen M. Progress in the preparation and application of modified biochar for improved contaminant removal from water and wastewater. Bioresour Technol. 2016;214:836–51.
17. Sizmur T, Fresno T, Akgül G, Frost H, Moreno-Jiménez E. Biochar modification to enhance sorption of inorganics from water. Bioresour Technol. 2017;246:34–47.
18. Rajapaksha AU, Chen SS, Tsang DCW, Zhang M, Vithanage M, Mandal S, et al. Engineered/designer biochar for contaminant removal/immobilization from soil and water: potential and implication of biochar modification. Chemosphere. Elsevier BV; 2016;148:276–91. Available from: https://doi.org/10.1016/j.chemosphere.2016.01.043
19. Wang J, Wang S. Preparation, modification and environmental application of biochar: a review. J Clean Prod. 2019;227:1002–22.
20. Lima I, Ro K, Reddy G, Boykin D, Klasson K. Efficacy of chicken litter and wood biochars and their activated counterparts in heavy metal clean up from wastewater. Agriculture. 2015;5:806–25.
21. Mondal S, Aikat K, Halder G. Biosorptive uptake of arsenic(V) by steam activated carbon from mung bean husk: equilibrium, kinetics, thermodynamics and modeling. Appl Water Sci. 2017;7:4479–95.
22. Rajapaksha AU, Vithanage M, Ahmad M, Seo DC, Cho JS, Lee SE, et al. Enhanced sulfamethazine removal by steam-activated invasive plant-derived biochar. J Hazard Mater. 2015;290:43–50. Available from: https://doi.org/10.1016/j.jhazmat.2015.02.046
23. Panwar NL, Pawar A. Influence of activation conditions on the physicochemical properties of activated biochar: a review. Biomass Convers Biorefinery. 2022;12:925–47.
24. Asadullah M, Jahan I, Ahmed MB, Adawiyah P, Malek NH, Rahman MS. Preparation of microporous activated carbon and its modification for arsenic removal from water. J Ind Eng Chem. 2014;20:887–96.
25. Lou K, Rajapaksha AU, Ok YS, Chang SX. Pyrolysis temperature and steam activation effects on sorption of phosphate on pine sawdust biochars in aqueous solutions. Chem Speciat Bioavailab. 2016;28:42–50.
26. Shim T, Yoo J, Ryu C, Park YK, Jung J. Effect of steam activation of biochar produced from a giant Miscanthus on copper sorption and toxicity. Bioresour Technol. 2015;197:85–90.
27. Chakraborty P, Banerjee S, Kumar S, Sadhukhan S, Halder G. Elucidation of ibuprofen uptake capability of raw and steam

activated biochar of Aegle marmelos shell: Isotherm, kinetics, thermodynamics and cost estimation. Process Saf Environ Prot. 2018;118:10–23.
28. Rajapaksha AU, Vithanage M, Zhang M, Ahmad M, Mohan D, Chang SX, et al. Pyrolysis condition affected sulfamethazine sorption by tea waste biochars. Bioresour Technol. 2014; 166:303–8.
29. Shao J, Zhang J, Zhang X, Feng Y, Zhang H, Zhang S, et al. Enhance SO2 adsorption performance of biochar modified by CO2 activation and amine impregnation. Fuel. 2018;224:138–46.
30. Xiong Z, Shihong Z, Haiping Y, Tao S, Yingquan C, Hanping C. Influence of NH3/CO2 modification on the characteristic of biochar and the CO2 capture. BioEnergy Res. 2013;6:1147–53.
31. Yu W, Lian F, Cui G, Liu Z. N-doping effectively enhances the adsorption capacity of biochar for heavy metal ions from aqueous solution. Chemosphere. 2018;193:8–16.
32. Zhang X, Zhang S, Yang H, Feng Y, Chen Y, Wang X, et al. Nitrogen enriched biochar modified by high temperature CO2-ammonia treatment: characterization and adsorption of CO2. Chem Eng J. 2014;257:20–7.
33. Li Y, Shao J, Wang X, Deng Y, Yang H, Chen H. Characterization of modified biochars derived from bamboo pyrolysis and their utilization for target component (furfural) adsorption. Energy Fuels. 2014;28:5119–27.
34. Shen W, Li Z, Liu Y. Surface chemical functional groups modification of porous carbon. Recent Patents Chem Eng. 2012;1:27–40.
35. Lyu H, Gao B, He F, Zimmerman AR, Ding C, Huang H, et al. Effects of ball milling on the physicochemical and sorptive properties of biochar: experimental observations and governing mechanisms. Environ Pollut. 2018;233:54–63.
36. Amusat SO, Kebede TG, Dube S, Nindi MM. Ball-milling synthesis of biochar and biochar–based nanocomposites and prospects for removal of emerging contaminants: a review. J Water Process Eng. 2021;41: 101993.
37. Foong SY, Liew RK, Yang Y, Cheng YW, Yek PNY, Wan Mahari WA, et al. Valorization of biomass waste to engineered activated biochar by microwave pyrolysis: progress, challenges, and future directions. Chem Eng J. 2020;389: 124401.
38. Lopez-Tenllado FJ, Motta IL, Hill JM. Modification of biochar with high-energy ball milling: development of porosity and surface acid functional groups. Bioresour Technol Reports. 2021;15: 100704.
39. Peterson SC, Jackson MA, Kim S, Palmquist DE. Increasing biochar surface area: Optimization of ball milling parameters. Powder Technol. 2012;228:115–20.
40. Huang J, Zimmerman AR, Chen H, Gao B. Ball milled biochar effectively removes sulfamethoxazole and sulfapyridine antibiotics from water and wastewater. Environ Pollut. 2020;258: 113809.
41. Ippolito JA, Strawn DG, Scheckel KG, Novak JM, Ahmedna M, Niandou MAS. Macroscopic and molecular investigations of copper sorption by a steam-activated biochar. J Environ Qual. 2012;41:1150–6.
42. Katiyar R, Patel AK, Nguyen TB, Singhania RR, Chen CW, Di DC. Adsorption of copper (II) in aqueous solution using biochars derived from Ascophyllum nodosum seaweed. Bioresour Technol. 2021;328: 124829.
43. Shan D, Deng S, Zhao T, Wang B, Wang Y, Huang J, et al. Preparation of ultrafine magnetic biochar and activated carbon for pharmaceutical adsorption and subsequent degradation by ball milling. J Hazard Mater. 2016;305:156–63.
44. Wei X, Wang X, Gao B, Zou W, Dong L. Facile ball-milling synthesis of CuO/biochar nanocomposites for efficient removal of reactive red 120. ACS Omega. 2020;5:5748–55.
45. Wongrod S, Simon S, van Hullebusch ED, Lens PNL, Guibaud G. Assessing arsenic redox state evolution in solution and solid phase during As(III) sorption onto chemically-treated sewage sludge digestate biochars. Bioresour Technol. 2019;275:232–8. Available from: https://doi.org/10.1016/j.biortech.2018.12.056
46. Seo D-C, Guo R, Lee D-H. Performance of alkaline impregnated biochar derived from rice hull for hydrogen sulfide removal from gas. Environ Eng Res. 2020;26: 200452.
47. Sun K, Tang J, Gong Y, Zhang H. Characterization of potassium hydroxide (KOH) modified hydrochars from different feedstocks for enhanced removal of heavy metals from water. Environ Sci Pollut Res. 2015;22:16640–51.
48. He R, Yuan X, Huang Z, Wang H, Jiang L, Huang J, et al. Activated biochar with iron-loading and its application in removing Cr (VI) from aqueous solution. Colloids Surfaces A Physicochem Eng Asp. 2019;579: 123642.
49. Mosa AA, El-Ghamry A, Al-Zahrani H, Selim E-M, El-Khateeb A. Chemically modified biochar derived from cotton stalks: characterization and assessing its potential for heavy metals removal from wastewater. Environ Biodivers Soil Secur. 2017;1:33–45. Available from: https://jenvbs.journals.ekb.eg/article_3214.html
50. Wang W, Ma X, Sun J, Chen J, Zhang J, Wang Y, et al. Adsorption of enrofloxacin on acid/alkali-modified corn stalk biochar. Spectrosc Lett. 2019;52:367–75.
51. Cerino-Córdova FJ, Díaz-Flores PE, García-Reyes RB, Soto-Regalado E, Gómez-González R, Garza-González MT, et al. Biosorption of Cu(II) and Pb(II) from aqueous solutions by chemically modified spent coffee grains. Int J Environ Sci Technol. 2013;10:611–22.
52. El-Sharkawy M, El-Naggar AH, Al-Huqail AA, Ghoneim AM. Acid-modified biochar impacts on soil properties and biochemical characteristics of crops grown in saline-sodic soils. Sustain. 2022;14:1–21.
53. Choudhary V, Philip L. Sustainability assessment of acid-modified biochar as adsorbent for the removal of pharmaceuticals and personal care products from secondary treated wastewater. J Environ Chem Eng. 2022;10: 107592.
54. Iriarte-Velasco U, Sierra I, Zudaire L, Ayastuy JL. Preparation of a porous biochar from the acid activation of pork bones. Food Bioprod Process. 2016;98:341–53.
55. Sahin O, Taskin MB, Kaya EC, Atakol O, Emir E, Inal A, et al. Effect of acid modification of biochar on nutrient availability and maize growth in a calcareous soil. Soil Use Manag. 2017;33:447–56.
56. Yakout SM, Daifullah AEHM, El-Reefy SA. Pore Structure characterization of chemically modified biochar derived from rice straw. Environ Eng Manag J. 2015;14:473–80.
57. Vithanage M, Rajapaksha AU, Zhang M, Thiele-Bruhn S, Lee SS, Ok YS. Acid-activated biochar increased sulfamethazine retention in soils. Environ Sci Pollut Res. 2015;22:2175–86.
58. Zhou N, Chen H, Feng Q, Yao D, Chen H, Wang H, et al. Effect of phosphoric acid on the surface properties and Pb(II) adsorption mechanisms of hydrochars prepared from fresh banana peels. J Clean Prod. 2017;165:221–30.
59. Sun L, Chen D, Wan S, Yu Z. Performance, kinetics, and equilibrium of methylene blue adsorption on biochar derived from eucalyptus saw dust modified with citric, tartaric, and acetic acids. Biores Technol. Elsevier Ltd; 2015;198:300–8. Available from: https://doi.org/10.1016/j.biortech.2015.09.026
60. Zhang D, Li Y, Sun A, Tong S, Su G, Jiang X, et al. Enhanced nitrobenzene reduction by modified biochar supported sulfidated nano zerovalent iron: comparison of surface modification methods. Sci Total Environ. 2019;694: 133701.
61. Mahdi Z, El Hanandeh A, Yu QJ. Preparation, characterization and application of surface modified biochar from date seed for

improved lead, copper, and nickel removal from aqueous solutions. J Environ Chem Eng. 2019;7: 103379.
62. Shen Y, Zhang N. Facile synthesis of porous carbons from silica-rich rice husk char for volatile organic compounds (VOCs) sorption. Bioresour Technol. 2019;282:294–300.
63. Petrović JT, Stojanović MD, Milojković JV, Petrović MS, Šoštarić TD, Laušević MD, et al. Alkali modified hydrochar of grape pomace as a perspective adsorbent of Pb2+ from aqueous solution. J Environ Manage. 2016;182:292–300.
64. Jin H, Capareda S, Chang Z, Gao J, Xu Y, Zhang J. Biochar pyrolytically produced from municipal solid wastes for aqueous As(V) removal: adsorption property and its improvement with KOH activation. Bioresour Technol. Elsevier BV; 2014;169:622–9. Available from: https://doi.org/10.1016/j.biortech.2014.06.103
65. Abdul Hamid SB, Chowdhury ZZ, Zain SM. Base catalytic approach: a promising technique for the activation of biochar for equilibrium sorption studies of Copper, Cu(II) ions in single solute system. Materials (Basel). 2014;7:2815–32.
66. Hussain M, Imran M, Abbas G, Shahid M, Iqbal M, Naeem MA, et al. A new biochar from cotton stalks for As (V) removal from aqueous solutions: its improvement with H3PO4 and KOH. Environ Geochem Health. 2020;42:2519–34.
67. Ding Z, Hu X, Wan Y, Wang S, Gao B. Removal of lead, copper, cadmium, zinc, and nickel from aqueous solutions by alkali-modified biochar: batch and column tests. J Ind Eng Chem. 2016;33:239–45. Available from: https://doi.org/10.1016/j.jiec.2015.10.007
68. Feng Z, Zhu L. Sorption of phenanthrene to biochar modified by base. Front Environ Sci Eng. 2018;12.
69. Guo JZ, Li B, Liu L, Lv K. Removal of methylene blue from aqueous solutions by chemically modified bamboo. Chemosphere. 2014;111:225–31.
70. Pietrzak R, Nowicki P, Kaźmierczak J, Kuszyńska I, Goscianska J, Przepiórski J. Comparison of the effects of different chemical activation methods on properties of carbonaceous adsorbents obtained from cherry stones. Chem Eng Res Des. 2014;92:1187–91.
71. Fan Y, Wang B, Yuan S, Wu X, Chen J, Wang L. Adsorptive removal of chloramphenicol from wastewater by NaOH modified bamboo charcoal. Bioresour Technol. 2010;101:7661–4.
72. Jung C, Boateng LK, Flora JRV, Oh J, Braswell MC, Son A, et al. Competitive adsorption of selected non-steroidal anti-inflammatory drugs on activated biochars: Experimental and molecular modeling study. Chem Eng J. 2015;264:1–9.
73. Jung C, Phal N, Oh J, Chu KH, Jang M, Yoon Y. Removal of humic and tannic acids by adsorption-coagulation combined systems with activated biochar. J Hazard Mater. 2015;300:808–14.
74. Kim E, Jung C, Han J, Her N, Park CM, Jang M, et al. Sorptive removal of selected emerging contaminants using biochar in aqueous solution. J Ind Eng Chem. 2016;36:364–71.
75. Liu P, Liu WJ, Jiang H, Chen JJ, Li WW, Yu HQ. Modification of bio-char derived from fast pyrolysis of biomass and its application in removal of tetracycline from aqueous solution. Bioresour Technol. Elsevier BV; 2012;121:235–40. Available from: https://doi.org/10.1016/j.biortech.2012.06.085
76. Tan G, Sun W, Xu Y, Wang H, Xu N. Sorption of mercury (II) and atrazine by biochar, modified biochars and biochar based activated carbon in aqueous solution. Bioresour Technol. 2016;211:727–35.
77. Cazetta AL, Vargas AMM, Nogami EM, Kunita MH, Guilherme MR, Martins AC, et al. NaOH-activated carbon of high surface area produced from coconut shell: kinetics and equilibrium studies from the methylene blue adsorption. Chem Eng J. 2011;174:117–25.
78. Jang HM, Kan E. Engineered biochar from agricultural waste for removal of tetracycline in water. Bioresour Technol. 2019;284:437–47.
79. Taha SM, Amer ME, Elmarsafy AE, Elkady MY. Adsorption of 15 different pesticides on untreated and phosphoric acid treated biochar and charcoal from water. J Environ Chem Eng. 2014;2:2013–25.
80. Sekulić MT, Pap S, Stojanović Z, Bošković N, Radonić J, Šolević KT. Efficient removal of priority, hazardous priority and emerging pollutants with Prunus armeniaca functionalized biochar from aqueous wastes: Experimental optimization and modeling. Sci Total Environ. 2018;613–614:736–50.
81. Zhao L, Zheng W, Mašek O, Chen X, Gu B, Sharma BK, et al. Roles of phosphoric acid in biochar formation: synchronously improving carbon retention and sorption capacity. J Environ Qual. 2017;46:393–401.
82. Hadjittofi L, Prodromou M, Pashalidis I. Activated biochar derived from cactus fibres - preparation, characterization and application on Cu(II) removal from aqueous solutions. Bioresour Technol. 2014;159:460–4.
83. Hadjittofi L, Pashalidis I. Uranium sorption from aqueous solutions by activated biochar fibres investigated by FTIR spectroscopy and batch experiments. J Radioanal Nucl Chem. 2015;304:897–904.
84. Peng P, Lang YH, Wang XM. Adsorption behavior and mechanism of pentachlorophenol on reed biochars: PH effect, pyrolysis temperature, hydrochloric acid treatment and isotherms. Ecol Eng. 2016;90:225–33. Available from: https://doi.org/10.1016/j.ecoleng.2016.01.039
85. Zhao N, Zhao C, Lv Y, Zhang W, Du Y, Hao Z, et al. Adsorption and coadsorption mechanisms of Cr(VI) and organic contaminants on H3PO4 treated biochar. Chemosphere. 2017;186:422–9.
86. Song Z, Lian F, Yu Z, Zhu L, Xing B, Qiu W. Synthesis and characterization of a novel MnOx-loaded biochar and its adsorption properties for Cu2+ in aqueous solution. Chem Eng J. 2014;242:36–42.
87. Wang H, Gao B, Wang S, Fang J, Xue Y, Yang K. Removal of Pb(II), Cu(II), and Cd(II) from aqueous solutions by biochar derived from KMnO4 treated hickory wood. Bioresour Technol. 2015;197:356–62.
88. Zhang Y, Fan J, Fu M, Ok YS, Hou Y, Cai C. Adsorption antagonism and synergy of arsenate(V) and cadmium(II) onto Fe-modified rice straw biochars. Environ Geochem Health. 2019;41:1755–66.
89. Wei Y, Wei S, Liu C, Chen T, Tang Y, Ma J, et al. Efficient removal of arsenic from groundwater using iron oxide nanoneedle array-decorated biochar fibers with high Fe utilization and fast adsorption kinetics. Water Res. 2019;167. Available from: https://doi.org/10.1016/j.watres.2019.115107
90. Kumar A, Gurian PL, Bucciarelli-Tieger RH, Mitchell-Blackwood J. Iron oxide - coated fibrous sorbents for arsenic removal. J / Am Water Work Assoc. 2008;100:151–64.
91. Zhang F, Wang X, Xionghui J, Ma L. Efficient arsenate removal by magnetite-modified water hyacinth biochar. Environ Pollut. 2016;216:575–83. Available from: https://doi.org/10.1016/j.envpol.2016.06.013
92. Wang S, Zhao M, Zhou M, Li YC, Wang J, Gao B, et al. Biochar-supported nZVI (nZVI/BC) for contaminant removal from soil and water: a critical review. J Hazard Mater. 2019;373:820–34.
93. Zhu S, Qu T, Irshad MK, Shang J. Simultaneous removal of Cd(II) and As(III) from co-contaminated aqueous solution by α-FeOOH modified biochar. Biochar. 2020;2:81–92.
94. Anyika C, Asri NAM, Majid ZA, Jaafar J, Yahya A. Batch sorption–desorption of As(III) from waste water by magnetic palm kernel shell activated carbon using optimized Box-Behnken design. Appl Water Sci. 2017;7:4573–91.

95. Lunge S, Singh S, Sinha A. Magnetic iron oxide (Fe3O4) nanoparticles from tea waste for arsenic removal. J Magn Magn Mater. 2014;356:21–31.
96. Dhoble RM, Maddigapu PR, Bhole AG, Rayalu S. Development of bark-based magnetic iron oxide particle (BMIOP), a bio-adsorbent for removal of arsenic (III) from water. Environ Sci Pollut Res. 2018;25:19657–74.
97. Jian X, Li S, Feng Y, Chen X, Kuang R, Li B, et al. Influence of Synthesis Methods on the High-Efficiency Removal of Cr(VI) from Aqueous Solution by Fe-Modified Magnetic Biochars. ACS Omega. 2020;5:31234–43.
98. Dong FX, Yan L, Zhou XH, Huang ST, Liang JY, Zhang WX, et al. Simultaneous adsorption of Cr(VI) and phenol by biochar-based iron oxide composites in water: performance, kinetics and mechanism. J Hazard Mater. 2021;416: 125930.
99. Yin Z, Liu Y, Liu S, Jiang L, Tan X, Zeng G, et al. Activated magnetic biochar by one-step synthesis: enhanced adsorption and coadsorption for 17β-estradiol and copper. Sci Total Environ. 2018;639:1530–42.
100. Wan Z, Cho DW, Tsang DCW, Li M, Sun T, Verpoort F. Concurrent adsorption and micro-electrolysis of Cr(VI) by nanoscale zerovalent iron/biochar/Ca-alginate composite. Environ Pollut. 2019;247:410–20. Available from: https://doi.org/10.1016/j.envpol.2019.01.047
101. Tang J, Zhao B, Lyu H, Li D. Development of a novel pyrite/biochar composite (BM-FeS2@BC) by ball milling for aqueous Cr(VI) removal and its mechanisms. J Hazard Mater. 2021;413: 125415.
102. Ren J, Li N, Li L, An JK, Zhao L, Ren NQ. Granulation and ferric oxides loading enable biochar derived from cotton stalk to remove phosphate from water. Bioresour Technol. 2015;178:119–25.
103. Phuong Tran TC, Nguyen TP, Nguyen TT, Le PC, Tran QB, Nguyen XC. Equilibrium single and co-adsorption of nutrients from aqueous solution onto aluminium-modified biochar. Case Stud Chem Environ Eng. 2022;5: 100181.
104. Meilani V, Lee JI, Kang JK, Lee CG, Jeong S, Park SJ. Application of aluminum-modified food waste biochar as adsorbent of fluoride in aqueous solutions and optimization of production using response surface methodology. Microporous Mesoporous Mater. 2021;312: 110764.
105. Wang S, Gao B, Li Y, Mosa A, Zimmerman AR, Ma LQ, et al. Manganese oxide-modified biochars: preparation, characterization, and sorption of arsenate and lead. Bioresour Technol. 2015;181:13–7.
106. Wang HY, Chen P, Zhu YG, Cen K, Sun GX. Simultaneous adsorption and immobilization of As and Cd by birnessite-loaded biochar in water and soil. Environ Sci Pollut Res. 2019;26:8575–84.
107. Tan X, Wei W, Xu C, Meng Y, Bai W, Yang W, et al. Manganese-modified biochar for highly efficient sorption of cadmium. Environ Sci Pollut Res. 2020;27:9126–34.
108. Zhu Y, Fan W, Feng W, Wang Y, Liu S, Dong Z, et al. Removal of EDTA-Cu(II) from water using synergistic fenton reaction-assisted adsorption by nanomanganese oxide-modified biochar: performance and mechanistic analysis. ACS ES&T Water. 2021;1:1302–12.
109. Xiao J, Hu R, Chen G, Xing B. Facile synthesis of multifunctional bone biochar composites decorated with Fe/Mn oxide micro-nanoparticles: physicochemical properties, heavy metals sorption behavior and mechanism. J Hazard Mater. 2020;399: 123067.
110. Zhou L, Huang Y, Qiu W, Sun Z, Liu Z, Song Z. Adsorption properties of nano-MnO2-biochar composites for copper in aqueous solution. Molecules. 2017;22.
111. Zhang A, Li X, Xing J, Xu G. Adsorption of potentially toxic elements in water by modified biochar: a review. J Environ Chem Eng. 2020;8:1–10.
112. Liao J, He X, Zhang Y, Zhu W, Zhang L, He Z. Bismuth impregnated biochar for efficient uranium removal from solution: adsorption behavior and interfacial mechanism. Sci Total Environ. 2022;819: 153145.
113. Xia D, Tan F, Zhang C, Jiang X, Chen Z, Li H, et al. ZnCl 2 -activated biochar from biogas residue facilitates aqueous As(III) removal. Appl Surf Sci. 2016;377:361–9.
114. Wang P, Tang L, Wei X, Zeng G, Zhou Y, Deng Y, et al. Synthesis and application of iron and zinc doped biochar for removal of p-nitrophenol in wastewater and assessment of the influence of co-existed Pb(II). Appl Surf Sci. 2017;392:391–401.
115. Shi Y, Shan R, Lu L, Yuan H, Jiang H, Zhang Y, et al. High-efficiency removal of Cr(VI) by modified biochar derived from glue residue. J Clean Prod. 2020;254: 119935.
116. Yu J, Jiang C, Guan Q, Ning P, Gu J, Chen Q, et al. Enhanced removal of Cr(VI) from aqueous solution by supported ZnO nanoparticles on biochar derived from waste water hyacinth. Chemosphere. 2018;195:632–40.
117. Gan C, Liu Y, Tan X, Wang S, Zeng G, Zheng B, et al. Effect of porous zinc-biochar nanocomposites on Cr(VI) adsorption from aqueous solution. RSC Adv. 2015;5:35107–15.
118. Zhao D, Luo Y, Feng Y yang, He Q ping, Zhang L sheng, Zhang K qiang, et al. Enhanced adsorption of phosphorus in soil by lanthanum-modified biochar: improving phosphorus retention and storage capacity. Environ Sci Pollut Res. 2021;28:68982–95.
119. Huang Y, He Y, Zhang H, Wang H, Li W, Li Y, et al. Selective adsorption behavior and mechanism of phosphate in water by different lanthanum modified biochar. J Environ Chem Eng. 2022;10: 107476.
120. Xu Q, Chen Z, Wu Z, Xu F, Yang D, He Q, et al. Novel lanthanum doped biochars derived from lignocellulosic wastes for efficient phosphate removal and regeneration. Bioresour Technol. 2019;289.
121. Xiao R, Wang JJ, Li R, Park J, Meng Y, Zhou B, et al. Enhanced sorption of hexavalent chromium [Cr(VI)] from aqueous solutions by diluted sulfuric acid-assisted MgO-coated biochar composite. Chemosphere. 2018;208:408–16.
122. Deng Y, Li X, Ni F, Liu Q, Yang Y, Wang M, et al. Synthesis of magnesium modified biochar for removing copper, lead and cadmium in single and binary systems from aqueous solutions: Adsorption mechanism. Water (Switzerland). 2021;13:1–15.
123. Cui X, Dai X, Khan KY, Li T, Yang X, He Z. Removal of phosphate from aqueous solution using magnesium-alginate/chitosan modified biochar microspheres derived from Thalia dealbata. Bioresour Technol. 2016;218:1123–32.
124. Fang C, Zhang T, Li P, Jiang RF, Wang YC. Application of magnesium modified corn biochar for phosphorus removal and recovery from swine wastewater. Int J Environ Res Public Health. 2014;11:9217–37. Available from: https://doi.org/10.3390/ijerph110909217
125. Chakhtouna H, Benzeid H, Zari N, Qaiss A el kacem, Bouhfid R. Functional CoFe2O4-modified biochar derived from banana pseudostem as an efficient adsorbent for the removal of amoxicillin from water. Sep Purif Technol. 2021;266:118592.
126. Wang Y, Wang XJ, Liu M, Wang X, Wu Z, Yang LZ, et al. Cr(VI) removal from water using cobalt-coated bamboo charcoal prepared with microwave heating. Ind Crops Prod. 2012;39:81–8.
127. Wang Y, Wang X, Wang X, Liu M, Wu Z, Yang L, et al. Adsorption of Pb(II) from aqueous solution to Ni-doped bamboo charcoal. J Ind Eng Chem. 2013;19:353–9.
128. Zhu D, Shao J, Li Z, Yang H, Zhang S, Chen H. Nano nickel embedded in N-doped CNTs-supported porous biochar for

adsorption-reduction of hexavalent chromium. J Hazard Mater. 2021;416.
129. Yan Y, Wang W, Peng Y, Xue K, Wang J, Xiao H. Heterogeneous NiS/NiSe/3D porous biochar for As removal from water by interface engineering-induced nickel lattice distortion. Sci Total Environ. 2021;776: 145874.
130. Wu J, Huang D, Liu X, Meng J, Tang C, Xu J. Remediation of As(III) and Cd(II) co-contamination and its mechanism in aqueous systems by a novel calcium-based magnetic biochar. J Hazard Mater. 2018;348:10–9. Available from: https://doi.org/10.1016/j.jhazmat.2018.01.011
131. Jung KW, Jeong TU, Kang HJ, Ahn KH. Characteristics of biochar derived from marine macroalgae and fabrication of granular biochar by entrapment in calcium-alginate beads for phosphate removal from aqueous solution. Bioresour Technol. 2016;211:108–16.
132. Liu T, Chen Z, Li Z, Chen G, Zhou J, Chen Y, et al. Rapid separation and efficient removal of Cd based on enhancing surface precipitation by carbonate-modified biochar. ACS Omega. 2021;6:18253–9.
133. Khan ZH, Gao M, Qiu W, Song Z. Properties and adsorption mechanism of magnetic biochar modified with molybdenum disulfide for cadmium in aqueous solution. Chemosphere. 2020;255: 126995.
134. Khan ZH, Gao M, Qiu W, Song Z. Mechanism of novel MoS2-modified biochar composites for removal of cadmium (II) from aqueous solutions. Environ Sci Pollut Res. 2021;28:34979–89.
135. Zhu H, Tan X, Tan L, Chen C, Alharbi NS, Hayat T, et al. Biochar derived from sawdust embedded with molybdenum disulfide for highly selective removal of pb2+. ACS Appl Nano Mater. 2018;1:2689–98.
136. Fang C, Zhang T, Li P, Jiang R, Wu S, Nie H, et al. Phosphorus recovery from biogas fermentation liquid by Ca-Mg loaded biochar. J Environ Sci (China). 2015;29:106–14.
137. Usman ARA, Ahmad M, El-Mahrouky M, Al-Omran A, Ok YS, Sallam AS, et al. Chemically modified biochar produced from conocarpus waste increases NO3 removal from aqueous solutions. Environ Geochem Health. 2016;38:511–21.
138. Shen B, Li G, Wang F, Wang Y, He C, Zhang M, et al. Elemental mercury removal by the modified bio-char from medicinal residues. Chem Eng . Elsevier BV; 2015;272:28–37. Available from: https://doi.org/10.1016/j.cej.2015.03.006
139. Wang X, Lian W, Sun X, Ma J, Ning P. Immobilization of NZVI in polydopamine surface-modified biochar for adsorption and degradation of tetracycline in aqueous solution. Front Environ Sci Eng. 2018;12.
140. Zhu Y, Dai W, Deng K, Pan T, Guan Z. Efficient removal of Cr(VI) from aqueous solution by Fe-Mn oxide-modified biochar. Water Air Soil Pollut. 2020;231:61.
141. Yin G, Song X, Tao L, Sarkar B, Sarmah AK, Zhang W, et al. Novel Fe-Mn binary oxide-biochar as an adsorbent for removing Cd(II) from aqueous solutions. Chem Eng J. 2020;389: 124465.
142. Yang T, Xu Y, Huang Q, Sun Y, Liang X, Wang L, et al. Adsorption characteristics and the removal mechanism of two novel Fe-Zn composite modified biochar for Cd(II) in water. Bioresour Technol. 2021;333: 125078.
143. Zhu N, Yan T, Qiao J, Cao H. Adsorption of arsenic, phosphorus and chromium by bismuth impregnated biochar: Adsorption mechanism and depleted adsorbent utilization. Chemosphere. 2016;164:32–40.
144. Hu B, Tang Y, Wang X, Wu L, Nong J, Yang X, et al. Cobalt-gadolinium modified biochar as an adsorbent for antibiotics in single and binary systems. Microchem J. 2021;166: 106235.
145. Mohan D, Kumar H, Sarswat A, Alexandre-Franco M, Pittman CU. Cadmium and lead remediation using magnetic oak wood and oak bark fast pyrolysis bio-chars. Chem Eng J. 2014;236:513–28.
146. Singh P, Sarswat A, Pittman CU, Mlsna T, Mohan D. Sustainable Low-Concentration Arsenite [As(III)] Removal in Single and Multicomponent Systems Using Hybrid Iron Oxide-Biochar Nanocomposite Adsorbents - A Mechanistic Study. ACS Omega. 2020;5:2575–93.
147. Agrafioti E, Kalderis D, Diamadopoulos E. Ca and Fe modified biochars as adsorbents of arsenic and chromium in aqueous solutions. J Environ Manage. 2014;146:444–50.
148. Zhou Y, Gao B, Zimmerman AR, Chen H, Zhang M, Cao X. Biochar-supported zerovalent iron for removal of various contaminants from aqueous solutions. Bioresour Technol. 2014;152:538–42.
149. Ramola S, Mishra T, Rana G, Srivastava RK. Characterization and pollutant removal efficiency of biochar derived from baggase, bamboo and tyre. Environ Monit Assess. 2014;186:9023–39.
150. Hu X, Ding Z, Zimmerman AR, Wang S, Gao B. Batch and column sorption of arsenic onto iron-impregnated biochar synthesized through hydrolysis. Water Res. 2015;68:206–16. Available from: https://doi.org/10.1016/J.WATRES.2014.10.009
151. Frišták V, Micháleková-Richveisová B, Víglašová E, Ďuriška L, Galamboš M, Moreno-Jiménéz E, et al. Sorption separation of Eu and As from single-component systems by Fe-modified biochar: kinetic and equilibrium study. J Iran Chem Soc. 2017;14:521–30.
152. Lata S, Prabhakar R, Adak A, Samadder SR. As(V) removal using biochar produced from an agricultural waste and prediction of removal efficiency using multiple regression analysis. Environ Sci Pollut Res. 2019;26:32175–88.
153. Alchouron J, Navarathna C, Chludil HD, Dewage NB, Perez F, Hassan EB, et al. Assessing South American Guadua chacoensis bamboo biochar and Fe3O4 nanoparticle dispersed analogues for aqueous arsenic(V) remediation. Sci Total Environ. 2020;706.
154. Di DC, Chen CW, Hung CM. Synthesis of magnetic biochar from bamboo biomass to activate persulfate for the removal of polycyclic aromatic hydrocarbons in marine sediments. Bioresour Technol. 2017;245:188–95.
155. Liu F, Zuo J, Chi T, Wang P, Yang B. Removing phosphorus from aqueous solutions by using iron-modified corn straw biochar. Front Environ Sci Eng. 2015;9:1066–75.
156. Harikishore Kumar Reddy D, Lee SM. Magnetic biochar composite: facile synthesis, characterization, and application for heavy metal removal. Colloids Surfaces A Physicochem Eng Asp. 2014;454:96–103.
157. Wang S, Gao B, Zimmerman AR, Li Y, Ma L, Harris WG, et al. Removal of arsenic by magnetic biochar prepared from pinewood and natural hematite. Bioresour Technol. Elsevier BV; 2015;175:391–5. Available from: https://doi.org/10.1016/j.biortech.2014.10.104
158. Han Z, Sani B, Mrozik W, Obst M, Beckingham B, Karapanagioti HK, et al. Magnetite impregnation effects on the sorbent properties of activated carbons and biochars. Water Res. 2015;70:394–403.
159. Samsuri AW, Sadegh-Zadeh F, Seh-Bardan BJ. Adsorption of As(III) and As(V) by Fe coated biochars and biochars produced from empty fruit bunch and rice husk. J Environ Chem Eng. Elsevier BV; 2013;1:981–8. Available from: https://doi.org/10.1016/j.jece.2013.08.009
160. Mubarak NM, Kundu A, Sahu JN, Abdullah EC, Jayakumar NS. Synthesis of palm oil empty fruit bunch magnetic pyrolytic char impregnating with FeCl3 by microwave heating technique. Biomass Bioenerg. 2014;61:265–75.
161. Zhang M, Gao B, Varnoosfaderani S, Hebard A, Yao Y, Inyang M. Preparation and characterization of a novel magnetic biochar

for arsenic removal. Bioresour Technol. 2013;130:457–62. Available from: https://doi.org/10.1016/J.BIORTECH.2012.11.132
162. Yoon K, Cho DW, Tsang DCW, Bolan N, Rinklebe J, Song H. Fabrication of engineered biochar from paper mill sludge and its application into removal of arsenic and cadmium in acidic water. Bioresour Technol. 2017;246:69–75.
163. Devi P, Saroha AK. Simultaneous adsorption and dechlorination of pentachlorophenol from effluent by Ni-ZVI magnetic biochar composites synthesized from paper mill sludge. Chem Eng J. 2015;271:195–203.
164. Yan J, Han L, Gao W, Xue S, Chen M. Biochar supported nanoscale zerovalent iron composite used as persulfate activator for removing trichloroethylene. Bioresour Technol. Elsevier BV; 2015;175:269–74. Available from: https://doi.org/10.1016/j.biortech.2014.10.103
165. Jung K-WW, Choi BH, Jeong T-UU, Ahn K-HH. Facile synthesis of magnetic biochar/Fe3O4 nanocomposites using electromagnetization technique and its application on the removal of acid orange 7 from aqueous media. Bioresour Technol. Elsevier BV; 2016;220:672–6. Available from: https://doi.org/10.1016/j.biortech.2016.09.035
166. Jung KW-. W, Hwang MJ-. J, Jeong TU-. U, Ahn KH-. H. A novel approach for preparation of modified-biochar derived from marine macroalgae: dual purpose electro-modification for improvement of surface area and metal impregnation. Bioresour Technol. 2015;191:342–5. Available from: https://doi.org/10.1016/j.biortech.2015.05.052
167. Zhang M, Gao B. Removal of arsenic, methylene blue, and phosphate by biochar/AlOOH nanocomposite. Chem Eng J. 2013;226:286–92. Available from: https://doi.org/10.1016/J.CEJ.2013.04.077
168. Qian W, Zhao AZ, Xu RK. Sorption of As(V) by aluminum-modified crop straw-derived biochars. Water Air Soil Pollut. 2013;224.
169. Wu C, Huang L, Xue SG, Huang YY, Hartley W, Cui M qian, et al. Arsenic sorption by red mud-modified biochar produced from rice straw. Environ Sci Pollut Res. 2017;24:18168–78.
170. Liang J, Li X, Yu Z, Zeng G, Luo Y, Jiang L, et al. Amorphous MnO2 modified biochar derived from aerobically composted swine manure for adsorption of Pb(II) and Cd(II). ACS Sustain Chem Eng. 2017;5:5049–58.
171. Wang MC, Sheng GD, Qiu YP. A novel manganese-oxide/biochar composite for efficient removal of lead(II) from aqueous solutions. Int J Environ Sci Technol. 2015;12:1719–26.
172. Trakal L, Michálková Z, Beesley L, Vítková M, Ouředníček P, Barceló AP, et al. AMOchar: amorphous manganese oxide coating of biochar improves its efficiency at removing metal(loid)s from aqueous solutions. Sci Total Environ. 2018;625:71–8. Available from: https://doi.org/10.1016/j.scitotenv.2017.12.267
173. Zhu N, Qiao J, Yan T. Arsenic immobilization through regulated ferrolysis in paddy field amendment with bismuth impregnated biochar. Sci Total Environ. 2019;648:993–1001.
174. Yan J, Xue Y, Long L, Zeng Y, Hu X. Adsorptive removal of As(V) by crawfish shell biochar: batch and column tests. Environ Sci Pollut Res. 2018;25:34674–83.
175. Zafar M, Van Vinh N, Behera SK, Park HS. Ethanol mediated As(III) adsorption onto Zn-loaded pinecone biochar: experimental investigation, modeling, and optimization using hybrid artificial neural network-genetic algorithm approach. J Environ Sci (China). 2017;54:114–25.
176. Yan L, Kong L, Qu Z, Li L, Shen G. Magnetic biochar decorated with ZnS nanocrytals for Pb (II) removal. ACS Sustain Chem Eng. 2015;3:125–32.
177. Van Vinh N, Zafar M, Behera SK, Park HS. Arsenic(III) removal from aqueous solution by raw and zinc-loaded pine cone biochar: equilibrium, kinetics, and thermodynamics studies. Int J Environ Sci Technol. 2015;12:1283–94.
178. Rodríguez-Romero JA, Mendoza-Castillo DI, Reynel-Ávila HE, De Haro-Del Rio DA, González-Rodríguez LM, Bonilla-Petriciolet A, et al. Preparation of a new adsorbent for the removal of arsenic and its simulation with artificial neural network-based adsorption models. J Environ Chem Eng. 2020;8.
179. Sun X, Guo P, Sun Y, Cui Y. Adsorption of hexavalent chromium by sodium alginate fiber biochar loaded with lanthanum. Materials (Basel). 2021;14.
180. Jung KW, Ahn KH. Fabrication of porosity-enhanced MgO/biochar for removal of phosphate from aqueous solution: application of a novel combined electrochemical modification method. Bioresour Technol. 2016;200:1029–32.
181. Jellali S, Diamantopoulos E, Haddad K, Anane M, Durner W, Mlayah A. Lead removal from aqueous solutions by raw sawdust and magnesium pretreated biochar: experimental investigations and numerical modelling. J Environ Manage. 2016;180:439–49.
182. Zhang M, Gao B, Yao Y, Xue Y, Inyang M. Synthesis of porous MgO-biochar nanocomposites for removal of phosphate and nitrate from aqueous solutions. Chem Eng J. 2012;210:26–32. Available from: https://doi.org/10.1016/j.cej.2012.08.052
183. Usman A, Sallam A, Al-Omran A, El-Naggar A, Alenazi K, Nadeem M, et al. Chemically modified biochar produced from conocarpus wastes: an efficient sorbent for Fe(II) removal from acidic aqueous solutions. Adsorpt Sci Technol. 2013;31:625–40.
184. Zhang XN, Mao GY, Jiao YB, Shang Y, Han RP. Adsorption of anionic dye on magnesium hydroxide-coated pyrolytic bio-char and reuse by microwave irradiation. Int J Environ Sci Technol. 2014;11:1439–48.
185. Lin L, Song Z, Khan ZH, Liu X, Qiu W. Enhanced As(III) removal from aqueous solution by Fe-Mn-La-impregnated biochar composites. Sci Total Environ. 2019;686:1185–93.
186. Liu X, Gao M, Qiu W, Khan ZH, Liu N, Lin L, et al. Fe–Mn–Ce oxide-modified biochar composites as efficient adsorbents for removing As(III) from water: adsorption performance and mechanisms. Environ Sci Pollut Res. 2019;26:17373–82.
187. Lin L, Qiu W, Wang D, Huang Q, Song Z, Chau HW. Arsenic removal in aqueous solution by a novel Fe-Mn modified biochar composite: characterization and mechanism. Ecotoxicol Environ Saf. 2017;144:514–21.
188. Guo J, Yan C, Luo Z, Fang H, Hu S, Cao Y. Synthesis of a novel ternary HA/Fe-Mn oxides-loaded biochar composite and its application in cadmium(II) and arsenic(V) adsorption. J Environ Sci (China). 2019;85:168–76.
189. Wang S, Gao B, Li Y. Enhanced arsenic removal by biochar modified with nickel (Ni) and manganese (Mn) oxyhydroxides. J Ind Eng Chem. 2016;37:361–5.
190. Oghbaei M, Mirzaee O. Microwave versus conventional sintering: a review of fundamentals, advantages and applications. J Alloys Compd. 2010;494:175–89.
191. Zubrik A, Matik M, Lovás M, Štefušová K, Danková Z, Hredzák S, et al. One-step microwave synthesis of magnetic biochars with sorption properties. Carbon Lett. 2018;26:31–42.
192. Luque R, Menéndez JA, Arenillas A, Cot J. Microwave-assisted pyrolysis of biomass feedstocks: the way forward? Energy Environ Sci. 2012;5:5481–8.
193. Jung KW, Jeong TU, Hwang MJ, Kim K, Ahn KH. Phosphate adsorption ability of biochar/Mg-Al assembled nanocomposites prepared by aluminum-electrode based electro-assisted modification method with MgCl2 as electrolyte. Bioresour Technol. 2015;198:603–10.
194. Peter A, Chabot B, Loranger E. Enhancing surface properties of softwood biochar by ultrasound assisted slow pyrolysis. IEEE Int Ultrason Symp IUS. 2019;2019-Octob:2477–80.
195. Luo M, Lin H, He Y, Li B, Dong Y, Wang L. Efficient simultaneous removal of cadmium and arsenic in aqueous solution

by titanium-modified ultrasonic biochar. Bioresour Technol. 2019;284:333–9.
196. He R, Peng Z, Lyu H, Huang H, Nan Q, Tang J. Synthesis and characterization of an iron-impregnated biochar for aqueous arsenic removal. Sci Total Environ. 2018;612:1177–86.
197. Bakshi S, Banik C, Rathke SJ, Laird DA. Arsenic sorption on zero-valent iron-biochar complexes. Water Res. Elsevier BV; 2018;137:153–63. Available from: https://doi.org/10.1016/j.watres.2018.03.021
198. Jimenez-Cordero D, Heras F, Alonso-Morales N, Gilarranz MA, Rodriguez JJ. Ozone as oxidation agent in cyclic activation of biochar. Fuel Process Technol. 2015;139:42–8.
199. Huff MD, Marshall S, Saeed HA, Lee JW. Surface oxygenation of biochar through ozonization for dramatically enhancing cation exchange capacity. Bioresour Bioprocess. 2018;5.
200. Zhao G, Li J, Ren X, Chen C, Wang X. Few-layered graphene oxide nanosheets as superior sorbents for heavy metal ion pollution management. Environ Sci Technol. 2011;45:10454–62.
201. Li Y, Song N, Wang K. Preparation and characterization of a novel graphene/biochar composite and its application as an adsorbent for Cd removal from aqueous solution. Korean J Chem Eng. 2019;36:678–87.
202. Chakraborty V, Das P, Roy PK. Graphene oxide–coated pyrolysed biochar from waste sawdust and its application for treatment of cadmium-containing solution: batch, fixed-bed column, regeneration, and mathematical modelling. Biomass Convers Biorefinery. 2021;1–12.
203. Inyang M, Gao B, Zimmerman A, Zhou Y, Cao X. Sorption and cosorption of lead and sulfapyridine on carbon nanotube-modified biochars. Environ Sci Pollut Res. 2015;22:1868–76.
204. Zhang MM, Liu YG, Li TT, Xu WH, Zheng BH, Tan XF, et al. Chitosan modification of magnetic biochar produced from Eichhornia crassipes for enhanced sorption of Cr(vi) from aqueous solution. RSC Adv. 2015;5:46955–64.
205. Zhou Y, Gao B, Zimmerman AR, Fang J, Sun Y, Cao X. Sorption of heavy metals on chitosan-modified biochars and its biological effects. Chem Eng J. Elsevier BV; 2013;231:512–8. Available from: https://doi.org/10.1016/j.cej.2013.07.036
206. Huang X, Liu Y, Liu S, Tan X, Ding Y, Zeng G, et al. Effective removal of Cr(VI) using β-cyclodextrin-chitosan modified biochars with adsorption/reduction bifuctional roles. RSC Adv. 2015;6:94–104.
207. Deng J, Liu Y, Liu S, Zeng G, Tan X, Huang B, et al. Competitive adsorption of Pb(II), Cd(II) and Cu(II) onto chitosan-pyromellitic dianhydride modified biochar. J Colloid Interface Sci. 2017;506:355–64.
208. Xiao F, Cheng J, Cao W, Yang C, Chen J, Luo Z. Removal of heavy metals from aqueous solution using chitosan-combined magnetic biochars. J Colloid Interface Sci. 2019;540:579–84.
209. Rawal A, Joseph SD, Hook JM, Chia CH, Munroe PR, Donne S, et al. Mineral-biochar composites: molecular structure and porosity. Environ Sci Technol. 2016;50:7706–14.
210. Yao C, Joseph S, Li L, Pan G, Lin Y, Munroe P, et al. Developing more effective enhanced biochar fertilisers for improvement of pepper yield and quality. pedosphere. Elsevier BV; 2015;25:703–12. Available from: https://doi.org/10.1016/s1002-0160(15)30051-5
211. Cai T, Liu X, Zhang J, Tie B, Lei M, Wei X, et al. Silicate-modified oiltea camellia shell-derived biochar: a novel and cost-effective sorbent for cadmium removal. J Clean Prod. 2021;281: 125390.
212. Ruan ZH, Wu JH, Huang JF, Lin ZT, Li YF, Liu YL, et al. Facile preparation of rosin-based biochar coated bentonite for supporting α-Fe2O3 nanoparticles and its application for Cr(vi) adsorption. J Mater Chem A. 2015;3:4595–603.
213. Ramola S, Belwal T, Li CJ, Wang YY, Lu HH, Yang SM, et al. Improved lead removal from aqueous solution using novel porous bentonite - and calcite-biochar composite. Sci Total Environ. 2020;709: 136171.
214. Din SU, Khan MS, Hussain S, Imran M, Haq S, Hafeez M, et al. Adsorptive mechanism of chromium adsorption on siltstone–nanomagnetite–biochar composite. J Inorg Organomet Polym Mater. 2021;31:1608–20.
215. Zhang J, Lu M, Wan J, Sun Y, Lan H, Deng X. Effects of pH, dissolved humic acid and Cu2+ on the adsorption of norfloxacin on montmorillonite-biochar composite derived from wheat straw. Biochem Eng J. 2018;130:104–12.
216. Fu C, Zhang H, Xia M, Lei W, Wang F. The single/co-adsorption characteristics and microscopic adsorption mechanism of biochar-montmorillonite composite adsorbent for pharmaceutical emerging organic contaminant atenolol and lead ions. Ecotoxicol Environ Saf. 2020;187: 109763.
217. Yakout SM. Monitoring the changes of chemical properties of rice straw-derived biochars modified by different oxidizing agents and their adsorptive performance for organics. Bioremediat J. 2015;19:171–82.
218. Wang F, Jin L, Guo C, Min L, Zhang P, Sun H, et al. Enhanced heavy metals sorption by modified biochars derived from pig manure. Sci Total Environ. 2021;786: 147595.
219. Jing XR, Wang YY, Liu WJ, Wang YK, Jiang H. Enhanced adsorption performance of tetracycline in aqueous solutions by methanol-modified biochar. Chem Eng J. 2014;248:168–74.
220. Roy P, Mondal NK, Bhattacharya S, Das B, Das K. Removal of arsenic(III) and arsenic(V) on chemically modified low-cost adsorbent: batch and column operations. Appl Water Sci. 2013;3:293–309. Available from: https://doi.org/10.1007/s13201-013-0082-5
221. Liu J, Huang Z, Chen Z, Sun J, Gao Y, Wu E. Resource utilization of swine sludge to prepare modified biochar adsorbent for the efficient removal of Pb(II) from water. J Clean Prod. 2020;257: 120322.
222. Kanwal F, Rehman R, Mahmud T, Anwar J, Ilyas R. Isothermal and thermodynamical modeling of chromium (III) adsorption by composites of polyaniline with rice husk and saw dust. J Chil Chem Soc. 2012;57:1058–63. Available from: https://doi.org/10.4067/S0717-97072012000100022
223. Lin C, Luo W, Luo T, Zhou Q, Li H, Jing L. A study on adsorption of Cr (VI) by modified rice straw: Characteristics, performances and mechanism. J Clean Prod. 2018;196:626–34.
224. Xiao Z, Zhang L, Wu L, Chen D. Adsorptive removal of Cu(II) from aqueous solutions using a novel macroporous bead adsorbent based on poly(vinyl alcohol)/sodium alginate/KMnO4 modified biochar. J Taiwan Inst Chem Eng. 2019;102:110–7.
225. Yin Z, Zhu L, Mo F, Li S, Hu D, Chu R, et al. Preparation of biochar grafted with amino-riched dendrimer by carbonization, magnetization and functional modification for enhanced copper removal. J Taiwan Inst Chem Eng. 2021;121:349–59.
226. Pathy A, Ray J, Paramasivan B. Challenges and opportunities of nutrient recovery from human urine using biochar for fertilizer applications. J Clean Prod. 2021;304.
227. Ma Y, Liu WJ, Zhang N, Li YS, Jiang H, Sheng GP. Polyethylenimine modified biochar adsorbent for hexavalent chromium removal from the aqueous solution. Bioresour Technol. 2014;169:403–8.
228. Zhou Q, Jiang X, Li X, Jia CQ, Jiang W. Preparation of high-yield N-doped biochar from nitrogen-containing phosphate and its effective adsorption for toluene. RSC Adv. 2018;8:30171–9.
229. Yang GX, Jiang H. Amino modification of biochar for enhanced adsorption of copper ions from synthetic wastewater. Water Res. 2014;48:396–405.
230. Medha I, Chandra S, Vanapalli KR, Samal B, Bhattacharya J, Das BK. (3-Aminopropyl)triethoxysilane and iron rice straw biochar composites for the sorption of Cr (VI) and Zn (II) using the extract of heavy metals contaminated soil. Sci Total Environ. 2021;771: 144764.

231. Takaya CA, Fletcher LA, Singh S, Anyikude KU, Ross AB. Phosphate and ammonium sorption capacity of biochar and hydrochar from different wastes. Chemosphere. 2016;145:518–27. Available from: https://doi.org/10.1016/j.chemosphere.2015.11.052
232. Zhang H, Voroney RP, Price GW, White AJ. Sulfur-enriched biochar as a potential soil amendment and fertiliser. Soil Res. 2017;55:93–9.
233. Brennan A, Moreno Jiménez E, Alburquerque JA, Knapp CW, Switzer C. Effects of biochar and activated carbon amendment on maize growth and the uptake and measured availability of polycyclic aromatic hydrocarbons (PAHs) and potentially toxic elements (PTEs). Environ Pollut. 2014;193:79–87.
234. Zhang XY, Wang QC, Zhang SQ, Sun XJ, Zhang ZS. Stabilization/solidification (S/S) of mercury-contaminated hazardous wastes using thiol-functionalized zeolite and Portland cement. J Hazard Mater. 2009;168:1575–80.
235. O'Connor D, Peng T, Li G, Wang S, Duan L, Mulder J, et al. Sulfur-modified rice husk biochar: a green method for the remediation of mercury contaminated soil. Sci Total Environ. 2018;621:819–26.
236. Hu H, Xi B, Tan W. Effects of sulfur-rich biochar amendment on microbial methylation of mercury in rhizosphere paddy soil and methylmercury accumulation in rice. Environ Pollut. 2021;286.
237. Hu X, Xue Y, Liu L, Zeng Y, Long L. Preparation and characterization of Na2S-modified biochar for nickel removal. Environ Sci Pollut Res. 2018;25:9887–95.
238. Yao Y, Gao B, Chen J, Zhang M, Inyang M, Li Y, et al. Engineered carbon (biochar) prepared by direct pyrolysis of Mg-accumulated tomato tissues: characterization and phosphate removal potential. Bioresour Technol. 2013;138:8–13.
239. Youngwilai A, Kidkhunthod P, Jearanaikoon N, Chaiprapa J, Supanchaiyamat N, Hunt AJ, et al. Simultaneous manganese adsorption and biotransformation by Streptomyces violarus strain SBP1 cell-immobilized biochar. Sci Total Environ. 2020;713: 136708.
240. Wang X, Guo Z, Hu Z, Zhang J. Recent advances in biochar application for water and wastewater treatment: a review. PeerJ. 2020;8: e9164.
241. Duan X, Zhang C, Srinivasakannan C, Wang X. Waste walnut shell valorization to iron loaded biochar and its application to arsenic removal. Resour Technol. 2017;3:29–36.
242. Shang MR, Liu YG, Liu SB, Zeng GM, Tan XF, Jiang LH, et al. A novel graphene oxide coated biochar composite: Synthesis, characterization and application for Cr(VI) removal. RSC Adv. 2016;6:85202–12.
243. Tang J, Lv H, Gong Y, Huang Y. Preparation and characterization of a novel graphene/biochar composite for aqueous phenanthrene and mercury removal. Bioresour Technol. 2015;196:355–63.
244. Inyang M, Gao B, Zimmerman A, Zhang M, Chen H. Synthesis, characterization, and dye sorption ability of carbon nanotube-biochar nanocomposites. Chem Eng J. 2014;236:39–46. Available from: https://doi.org/10.1016/j.cej.2013.09.074
245. Ghaffar A, Younis MN. Adsorption of organic chemicals on graphene coated biochars and its environmental implications. Green Process Synth. 2014;3:479–87.
246. Zhang M, Gao B, Yao Y, Xue Y, Inyang M. Synthesis, characterization, and environmental implications of graphene-coated biochar. Sci Total Environ. 2012;435–436:567–72.
247. Chen L, Chen XL, Zhou CH, Yang HM, Ji SF, Tong DS, et al. Environmental-friendly montmorillonite-biochar composites: facile production and tunable adsorption-release of ammonium and phosphate. J Clean Prod. 2017;156:648–59.
248. Ismadji S, Tong DS, Soetaredjo FE, Ayucitra A, Yu WH, Zhou CH. Bentonite hydrochar composite for removal of ammonium from Koi fish tank. Appl Clay Sci. 2016;119:146–54.
249. Zhang M, Gao B, Yao Y, Inyang M. Phosphate removal ability of biochar/MgAl-LDH ultra-fine composites prepared by liquid-phase deposition. Chemosphere. 2013;92:1042–7.
250. Yao Y, Gao B, Fang J, Zhang M, Chen H, Zhou Y, et al. Characterization and environmental applications of clay-biochar composites. Chem Eng J. 2014;242:136–43.
251. Huff MD, Lee JW. Biochar-surface oxygenation with hydrogen peroxide. J Environ Manage. 2016;165:17–21.
252. Zuo XJ, Liu Z, Chen MD. Effect of H2O2 concentrations on copper removal using the modified hydrothermal biochar. Bioresour Technol. 2016;207:262–7.
253. Xue Y, Gao B, Yao Y, Inyang M, Zhang M, Zimmerman AR, et al. Hydrogen peroxide modification enhances the ability of biochar (hydrochar) produced from hydrothermal carbonization of peanut hull to remove aqueous heavy metals: batch and column tests. Chem Eng J. 2012;200–202:673–80.
254. Frankel ML, Bhuiyan TI, Veksha A, Demeter MA, Layzell DB, Helleur RJ, et al. Removal and biodegradation of naphthenic acids by biochar and attached environmental biofilms in the presence of co-contaminating metals. Bioresour Technol. 2016;216:352–61.
255. Dalahmeh S, Ahrens L, Gros M, Wiberg K, Pell M. Potential of biochar filters for onsite sewage treatment: adsorption and biological degradation of pharmaceuticals in laboratory filters with active, inactive and no biofilm. Sci Total Environ. 2018;612:192–201.
256. Dada AO. Langmuir, Freundlich, Temkin and Dubinin-Radushkevich isotherms studies of equilibrium sorption of Zn 2+ unto phosphoric acid modified rice husk. IOSR J Appl Chem. 2012;3:38–45.
257. Ayawei N, Ebelegi AN, Wankasi D. Modelling and interpretation of adsorption isotherms. Guo W, editor. J Chem. Hindawi; 2017;2017:3039817. Available from: https://doi.org/10.1155/2017/3039817
258. Foo KY, Hameed BH. Insights into the modeling of adsorption isotherm systems. Chem Eng J. 2010;156:2–10.
259. Mondal NK, Samanta A, Chakraborty S, Shaikh WA. Enhanced chromium(VI) removal using banana peel dust: isotherms, kinetics and thermodynamics study. Sustain Water Resour Manag. Springer Science and Business Media LLC; 2017;4:489–97. Available from: https://doi.org/10.1007/s40899-017-0130-7
260. Tan KL, Hameed BH. Insight into the adsorption kinetics models for the removal of contaminants from aqueous solutions. J Taiwan Inst Chem Eng. 2017;74:25–48.
261. Lin J, Wang L. Comparison between linear and non-linear forms of pseudo-first-order and pseudo-second-order adsorption kinetic models for the removal of methylene blue by activated carbon. Front Environ Sci Eng China. 2009;3:320–4.
262. Lima EC, Gomes AA, Tran HN. Comparison of the nonlinear and linear forms of the van't Hoff equation for calculation of adsorption thermodynamic parameters (ΔS° and ΔH°). J Mol Liq. 2020;311.
263. Liu C, Zhang HX. Modified-biochar adsorbents (MBAs) for heavy-metal ions adsorption: a critical review. J Environ Chem Eng. 2022;10: 107393.
264. Liu L, Liu X, Wang D, Lin H, Huang L. Removal and reduction of Cr(VI) in simulated wastewater using magnetic biochar prepared by co-pyrolysis of nano-zero-valent iron and sewage sludge. J Clean Prod. 2020;257: 120562.
265. Li H, Dong X, da Silva EB, de Oliveira LM, Chen Y, Ma LQ. Mechanisms of metal sorption by biochars: biochar characteristics and modifications. Chemosphere. 2017;178:466–78.
266. Sharma PK, Kumar R, Singh RK, Sharma P, Ghosh A. Review on arsenic removal using biochar-based materials. Groundw Sustain Dev. 2022;17: 100740.
267. Yin G, Tao L, Chen X, Bolan NS, Sarkar B, Lin Q, et al. Quantitative analysis on the mechanism of Cd2+ removal by MgCl2-modified biochar in aqueous solutions. J Hazard Mater. 2021;420: 126487.

268. Cheng N, Wang B, Wu P, Lee X, Xing Y, Chen M, et al. Adsorption of emerging contaminants from water and wastewater by modified biochar: a review. Environ Pollut. 2021;273: 116448.
269. Chen T, Luo L, Deng S, Shi G, Zhang S, Zhang Y, et al. Sorption of tetracycline on H3PO4 modified biochar derived from rice straw and swine manure. Bioresour Technol. 2018;267: 431–7.
270. Liu J, Zhou B, Zhang H, Ma J, Mu B, Zhang W. A novel Biochar modified by chitosan-Fe/S for tetracycline adsorption and studies on site energy distribution. Bioresour Technol. 2019;294: 122152.
271. Li R, Wang Z, Guo J, Li Y, Zhang H, Zhu J, et al. Enhanced adsorption of ciprofloxacin by KOH modified biochar derived from potato stems and leaves. Water Sci Technol. 2018;77: 1127–36.
272. Reguyal F, Sarmah AK. Adsorption of sulfamethoxazole by magnetic biochar: effects of pH, ionic strength, natural organic matter and 17α-ethinylestradiol. Sci Total Environ. 2018;628–629: 722–30.
273. Dong X, He L, Hu H, Liu N, Gao S, Piao Y. Removal of 17B-estradiol by using highly adsorptive magnetic biochar nanoparticles from aqueous solution. Chem Eng J. 2018;352: 371–9.
274. Tao H yu, Ge H, Shi J, Liu X, Guo W, Zhang M, et al. The characteristics of oestrone mobility in water and soil by the addition of Ca-biochar and Fe–Mn-biochar derived from Litchi chinensis Sonn. Environ Geochem Health. 2020;42:1601–15.
275. Rong X, Xie M, Kong L, Natarajan V, Ma L, Zhan J. The magnetic biochar derived from banana peels as a persulfate activator for organic contaminants degradation. Chem Eng J. 2019;372:294–303.
276. Heo J, Yoon Y, Lee G, Kim Y, Han J, Park CM. Enhanced adsorption of bisphenol A and sulfamethoxazole by a novel magnetic CuZnFe2O4–biochar composite. Bioresour Technol. 2019;281:179–87.
277. Sun P, Li Y, Meng T, Zhang R, Song M, Ren J. Removal of sulfonamide antibiotics and human metabolite by biochar and biochar/H2O2 in synthetic urine. Water Res. 2018;147:91–100.
278. Guo X, Dong H, Yang C, Zhang Q, Liao C, Zha F, et al. Application of goethite modified biochar for tylosin removal from aqueous solution. Colloids Surfaces A Physicochem Eng Asp. 2016;502:81–8.
279. Paunovic O, Pap S, Maletic S, Taggart MA, Boskovic N, Turk SM. Ionisable emerging pharmaceutical adsorption onto microwave functionalised biochar derived from novel lignocellulosic waste biomass. J Colloid Interface Sci. 2019;547:350–60.
280. dos Santos Lins PV, Henrique DC, Ide AH, de Paiva e Silva Zanta CL, Meili L. Evaluation of caffeine adsorption by MgAl-LDH/biochar composite. Environ Sci Pollut Res. 2019;26:31804–11.
281. Peiris C, Gunatilake SR, Mlsna TE, Mohan D, Vithanage M. Biochar based removal of antibiotic sulfonamides and tetracyclines in aquatic environments: a critical review. Bioresour Technol. 2017;246:150–9.
282. Wang L, O'Connor D, Rinklebe J, Ok YS, Tsang DCW, Shen Z, et al. Biochar aging: mechanisms, physicochemical changes, assessment, and implications for field applications. Environ Sci Technol. 2020;54:14797–814.
283. Shen Z, Hou D, Zhao B, Xu W, Ok YS, Bolan NS, et al. Stability of heavy metals in soil washing residue with and without biochar addition under accelerated ageing. Sci Total Environ. 2018;619–620:185–93.
284. Wang L, Bolan NS, Tsang DCW, Hou D. Green immobilization of toxic metals using alkaline enhanced rice husk biochar: effects of pyrolysis temperature and KOH concentration. Sci Total Environ. 2020;720: 137584.
285. Rechberger MV, Kloss S, Wang SL, Lehmann J, Rennhofer H, Ottner F, et al. Enhanced Cu and Cd sorption after soil aging of woodchip-derived biochar: what were the driving factors? Chemosphere. 2019;216:463–71.
286. Raeisi S, Motaghian H, Hosseinpur AR. Effect of the soil biochar aging on the sorption and desorption of Pb2+ under competition of Zn2+ in a sandy calcareous soil. Environ Earth Sci. 2020;79.
287. Huang X, Lyu P, Li L, Xie J, Zhu C. Effect of three aging processes on physicochemical and As(V) adsorption properties of Ce/Mn-modified biochar. Environ Res. 2022;214: 113839.
288. Wang Z, Geng C, Bian Y, Zhang G, Zheng C, An C. Effect of oxidative aging of biochar on relative distribution of competitive adsorption mechanism of Cd2+ and Pb2+. Sci Rep. 2022;12:11308.
289. Cui L, Fan Q, Sun J, Quan G, Yan J, Hina K, et al. Changes in surface characteristics and adsorption properties of 2,4,6-trichlorophenol following Fenton-like aging of biochar. Sci Rep. 2021;11:4293.
290. Chang R, Sohi SP, Jing F, Liu Y, Chen J. A comparative study on biochar properties and Cd adsorption behavior under effects of ageing processes of leaching, acidification and oxidation. Environ Pollut. 2019;254: 113123.
291. Woolf D, Amonette JE, Street-Perrott FA, Lehmann J, Joseph S. Sustainable biochar to mitigate global climate change. Nat Commun. 2010;1. Available from: https://doi.org/10.1038/ncomms1053
292. Martin SM, Kookana RS, Van Zwieten L, Krull E. Marked changes in herbicide sorption-desorption upon ageing of biochars in soil. J Hazard Mater. 2012;231–232:70–8.
293. Ren X, Sun H, Wang F, Zhang P, Zhu H. Effect of aging in field soil on biochar's properties and its sorption capacity. Environ Pollut. 2018;242:1880–6.
294. Jones DL, Edwards-Jones G, Murphy DV. Biochar mediated alterations in herbicide breakdown and leaching in soil. Soil Biol Biochem. 2011;43:804–13.
295. Li H, Ye X, Geng Z, Zhou H, Guo X, Zhang Y, et al. The influence of biochar type on long-term stabilization for Cd and Cu in contaminated paddy soils. J Hazard Mater. 2016;304:40–8.
296. Inyang M, Dickenson E. The potential role of biochar in the removal of organic and microbial contaminants from potable and reuse water: a review. Chemosphere. 2015;134:232–40.
297. Liu C, Wang W, Wu R, Liu Y, Lin X, Kan H, et al. Preparation of acid- and alkali-modified biochar for removal of methylene blue pigment. ACS Omega. 2020;5:30906–22.
298. Kumar A, Bhattacharya T, Mukherjee S, Sarkar B. A perspective on biochar for repairing damages in the soil–plant system caused by climate change-driven extreme weather events. Biochar. 2022;4:1–23.
299. Kumar A, Nagar S, Anand S. Climate change and existential threats. Glob Clim Chang. 2021;1–31.